Paleo-fluids characterization and fluid flow modelling along a regional transect in Northern United Arab Emirates

Callot, J.P.; Breesch, L.; Guilhaumou, N.; Roure, F.; Swennen, R.; Vilasie, N.

published in
Arabian Journal of Geosciences
2010

DOI (link to publisher)
10.1007/s12517-010-0233-z

document version
Publisher's PDF, also known as Version of record

Arab J Geosci (2010) 3:413–437
DOI 10.1007/s12517-010-0233-z

ORIGINAL PAPER

Paleo-fluids characterisation and fluid flow modelling along a regional transect in Northern United Arab Emirates (UAE)

Jean-Paul Callot · Liesbeth Breesch · Nicole Guilhaumou · François Roure · Rudy Swennen · Nadège Vilasi

Received: 31 March 2010 / Accepted: 1 November 2010 / Published online: 16 November 2010

Abstract In the Northern Emirates, Jurassic and Lower Cretaceous platform carbonates of the Musandam para-utochthonous units are tectonically overlain by siliciclastic units of the Hawasina–Sumeini allochthon, which derive from the former paleo-slope domain and a more distal basinal portion of the Arabian margin of the Tethys, respectively. All these tectonic units display numerous evidences of paleo-fluid circulations, accounting for dolomitisation and recrystallisation of the rock matrix (Musandam Platform units), as well as cementation of fractures. Polymict breccias of Upper Cretaceous Ausaq Formation which underlay the sole thrust of the Hawasina–Sumeini allochthon also record episodes of hydraulic fracturing, whereas fluid inclusion data indicate precipitation at high temperature in relation to paleo-fluid flow. Petrography of thin-sections (conventional and cathodoluminescence microscopic techniques) as well as fluid inclusion and stable isotopes analyses, were combined with micro-tectonic studies. These analytical data document (1) the paragenetic sequence of diagenetic products for the Musandam Platform (which constitutes a carbonate reservoir analogue) and Sumeini units of the Dibba Zone, as well as (2) the nature of the paleo-fluids circulating along fractures and the sole thrust of the Hawasina–Sumeini allochthon. The main results of this petrographic approach are qualitative, evidencing (1) the rapid and vertical transfer of hot fluids in the vicinity of the former slope to platform transition, accounting for episodes of hydrothermal dolomitisation, as well as (2) early (i.e. pre-orogenic) and late (i.e. post-orogenic) episodes of emersion of the carbonate units, accounting for additional interactions with meteoric fluids and karstification. In order to better link these diagenetic events with the overall burial, thermal and kinematic evolution of the Arabian margin, basin modelling with Ceres2D, including fluid flow and pore-fluid pressure modelling, was subsequently performed along a regional transect (D4) located in the vicinity of the samples localities and cross-cutting the Northern Oman Mountains from Dibba in the east up to the Arabian Gulf in the west. New subsurface constraints provided by deep seismic profiles were used to constrain the architecture of the cross-section, and to test various hypotheses on the

J.-P. Callot (✉) · L. Breesch · F. Roure · N. Vilasi
IFP Energies Nouvelles,
1-4 avenue de Bois Préau Rueil Malmaison Cedex,
92852, Paris, France
e-mail: J-Paul.Callot@ifpenergiesnouvelles.fr

L. Breesch · R. Swennen · N. Vilasi
KU Leuven,
Leuven, Belgium

N. Guilhaumou
LMCM, CNRS, Museum National d'Histoire Naturelle,
Paris, France

F. Roure
VU Amsterdam,
Amsterdam, the Netherlands

Present Address:
L. Breesch
University of Copenhagen,
Copenhagen, Denmark

Present Address:
N. Vilasi
StatoilHydro ASA,
Stavanger, Norway

lateral and vertical connection, timing and hydrodynamic behaviour of the faults. This Ceres basin modelling also provides new quantitative estimates of the paleo-fluid pathways, of the timing and velocities of the fluid transfers and of the evolution of pore-fluid pressures. Ultimately, this integration of petrographic studies on surface samples and coupled kinematic and fluid flow basin modelling provides an updated scenario for the succession of tectonically controlled episodes of fluid rock interactions, namely dolomitisation and karstification recorded in the Mesozoic platform carbonates of the Northern Emirates.

Keywords United Arab Emirates · Paleo-fluids characterisation · Fluid flow modelling · Ceres2D · Diagenesis

Introduction

Paleo-fluid flow is known to impact the reservoir properties of both carbonates and sandstones during successive geodynamic and tectonic stages involved in the long-lasting evolution of foreland fold-and-thrust belts (e.g. Roure et al. 2005, 2009, 2010 and reference therein). For instance, meteoric water can interact with the rock matrix during the early stages of plate convergence when foreland flexuring leads to emersion of a forebulge secondary porosity development in the foreland basin and eventually local karstification. Alternatively, hydraulic fracturing and thrusting can restore vertical permeabilities and allow deep basinal fluids to enter shallower reservoirs, resulting in rapid cementation or dissolution events, controlled by the chemistry (salinity, Mg content, pCO_2), the fluid temperatures, and the mineralogy of the rock matrix.

A workflow coupling petrographic and modelling studies has been recently developed by IFP New Energies (formerly the French Institute of Petroleum) and academic institutions in the scope of the Sub-Thrust Reservoir APpraisal research consortium (SUBTRAP project; Swennen et al. 2000, 2004; Van Geet et al. 2002; Benchilla et al. 2003; Ferket et al. 2003, 2004; Roure et al. 2005; Vandeginste et al. 2005; Roure 2008; Vilasi et al. 2009). Already tested in numerous thrust belts around the world, this integrated methodology is applied here to the study of both reservoir analogues and exploration risk assessment in the foothills of the Northern Emirates. Analytical studies were focused on Jurassic to Lower Cretaceous carbonates of the Musandam and Thamama groups and Upper Cretaceous breccias of the Ausaq Formation, which are cropping out in the Musandam unit and Dibba Zone, respectively. Ceres basin modelling (e.g. Schneider 2003) was applied on the regional traverse D4, in the vicinity of the sampled localities (Callot and Roure 2007). This geotraverse was compiled by integration of surface geology with deep seismic data recently recorded by Western-Geco on behalf of the Ministry of Energy of the Emirates (Styles et al. 2006; Tarapoanca et al. 2010 this volume). Based on the main results of this project, some of which have already been described in previous publications (e.g. Breesch 2008; Breesch et al. 2006, 2009, 2010a, b; Roure et al. 2010) this paper first documents the successive/alternating episodes of interaction between meteoric and/or hydrothermal fluids with the rock matrix, as evidenced by field and petrographic studies. These analytical data are further discussed and compared with results of basin modelling, in order to better understand the spatial and temporal changes observed in the regional fluid flow and its incidence on diagenetic processes operating in an open system.

Regional geological background

Location of the study and sampling area

The study area is located in the Northern Emirates (Figs. 1 and 2). It extends from the Gulf of Oman in the east and the Arabian Gulf in the west, and constitutes the northernmost part of the Oman Range, a fold-and-thrust belt that developed during the Late Cretaceous and Early Cenozoic along the eastern margin of the Arabian plate, and connects northward to the Makran and Zagros compressional systems. Most of the field work and sampling aimed at studying Jurassic carbonates of the Musandam Group and Lower Cretaceous carbonates of the Thamama Group (up to Aptian) along the seismic transect D4 (Fig. 3a, Roure et al. 2006). This transect is complemented by the study of cemented fractures observed in these series in various localities of the Musandam Platform unit (Fig. 2), slightly north of transect D4. Additional samples were also collected along the profile itself, i.e. in the Dibba zone, where paleo-slope (Sumeini) units and more distal basinal (Hawasina) units are locally exposed between the Arabian foreland and the Musandam Platform carbonate unit in the one hand, and the Semail Ophiolite (paleo-oceanic unit) in the other hand (Figs. 2 and 3b).

Main lithostratigraphic and tectonic units

The main tectono-statigraphic units cropping out in the Northern Emirates comprise, from west to east and from bottom to top (Figs. 2 and 3):

1. A foreland autochthon, made up of the Precambrian substratum, a Paleozoic to Lower Cretaceous (up to Aptian) carbonate platform, which belongs to the former passive margin of the Arabian plate (Eilrich

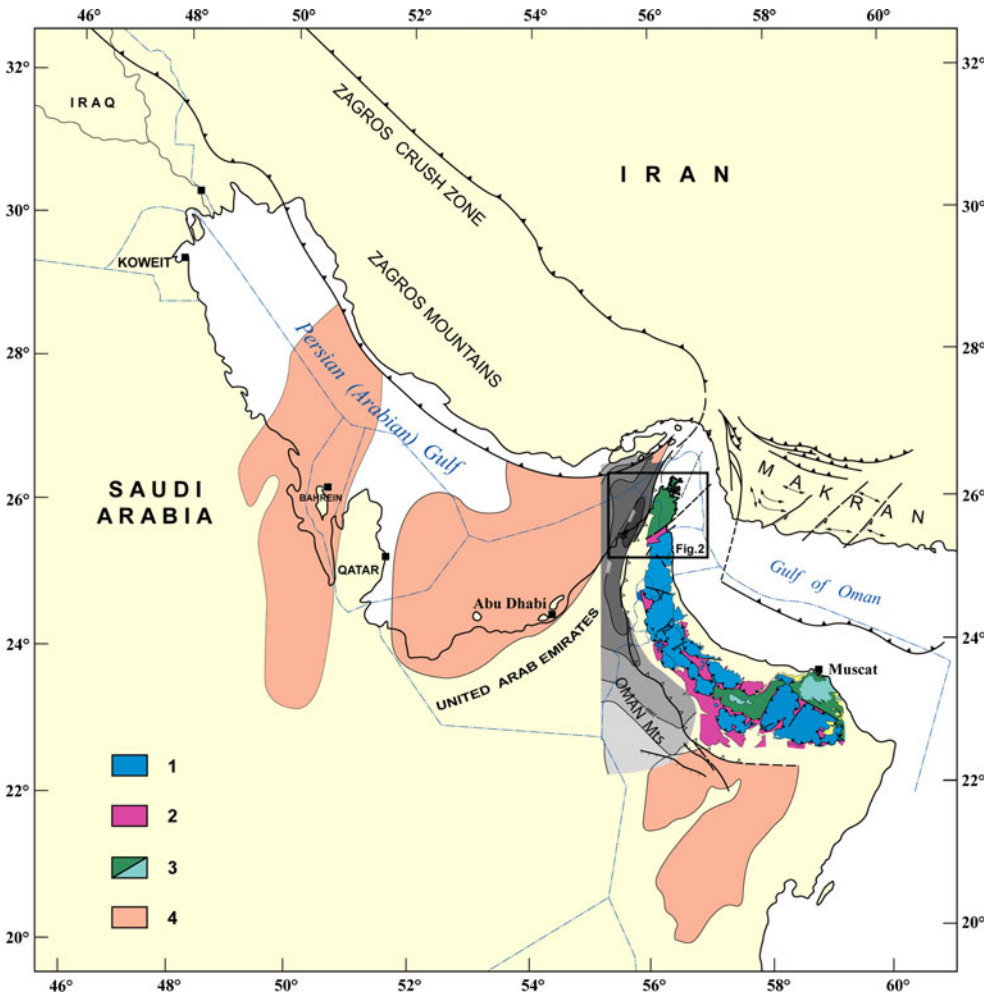

Fig. 1 Location of the Northern Emirates and Oman Range in the framework of the Arabian plate and Zagros Mountains. *1* Semail Ophiolite; *2* Hawasina and Sumeini allochtons; *3* Paleozoic to Mesozoic autochtonous sedimentary cover; *4* Hormuz Precambrian to Cambrian salt. *Grey levels* localise isobaths of the depth to the foreland base

and Grötsch 2003), and an overlying Late Cretaceous to Neogene flexural sequence (Fig. 3a).

2. A frontal triangle zone, which developed during the Neogene (Fig. 3a), and where deep duplexes made up of platform carbonates are progressively stacked in an out-of-sequence mode, resulting in the refolding of the former sole thrust of the Hawasina–Sumeini allochthon (Fig. 3a and b).
3. The Dibba Zone, which comprises a complex stack of Hawasina units, made up of Triassic to Cretaceous basinal series, and of Sumeini units, made up of dominantly Lower to Middle Cretaceous paleo-slope units (Fig. 3b, Graham 1980a, 1980b; Lippard et al. 1982; Watts and Garrison 1986; Robertson et al. 1990; Watts 1990; Watts and Blome 1990; Eilrich and Grötsch 2003). Most of this part of the Omani belt was probably deformed during the Late Cretaceous, soon after the thrust emplacement of the Semail Ophiolite on top of the Hawasina basinal domain (Glennie et al. 1974; Dunne et al. 1990). Underthrusted foreland platform units are likely to extend below most of the Dibba Zone, and may constitute additional targets for exploration (Fig. 2).

Overall geodynamic background and tectonic agenda

Tethyan rifting affected the eastern border of the Arabian plate during the Permian, and accounts for the subsequent development of a passive margin during the Mesozoic. Shallow platform carbonate sedimentation persisted over most of the current autochthonous and parautochthonous domains of the Northern Emirates until the Aptian. Deeper water, dominantly shaly facies of the Aruma Group was deposited in the Late Cretaceous foredeep basin, which developed as a flexural response of the Arabian lithosphere to the obduction of the Semail Ophiolite (Patton and O'Connor 1986, 1988; Warburton et al. 1990). This occurred synchronously with a progressive stacking of the Hawasina–Sumeini units in a westward propagating accretionary wedge.

In the foreland, a sedimentary hiatus or small erosional event is observed during the Mid-Cretaceous between the

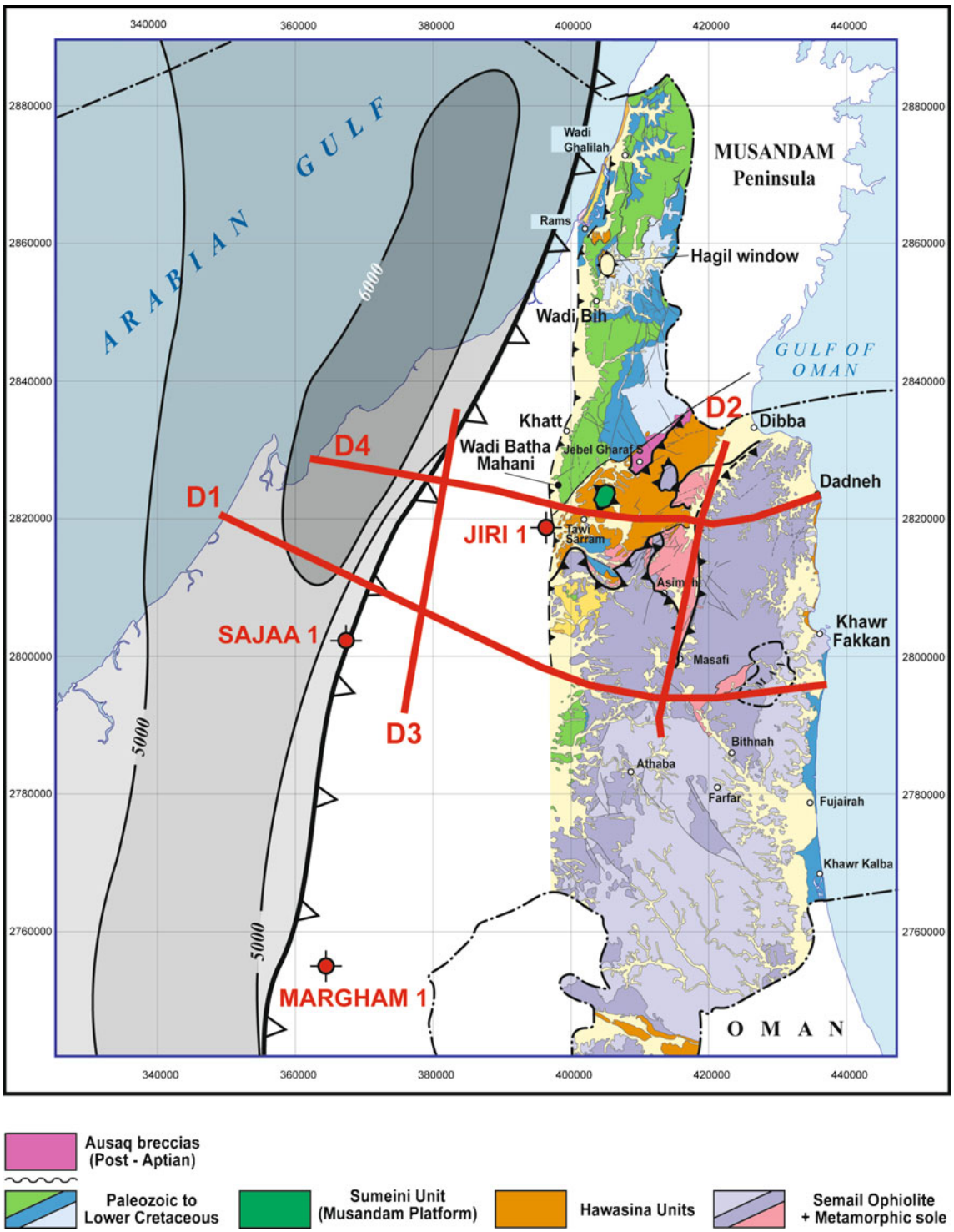

Fig. 2 Geologic map of the Northern Emirates, outlining the location of the studied outcrops, the wells, the D1 to D4 regional traverses (Ceres modelling along D4) and Apatite Fission Track localities. *Grey levels* localise isobaths of the depth to the foreland base

youngest platform series and the oldest flexural sequences. This hiatus is commonly interpreted as a short, local episode of emersion that would record the inception and progressive migration of the forebulge during the Turonian–Campanian.

In the southeastern part of the Munsandam unit however, polymictic breccias of the Ausaq Formation rest unconformably on top of Lower Cretaceous, Jurassic, Triassic and even Permian series, and are tectonically overlain by the Hawasina–Sumeini allochthonous units of the Dibba Zone

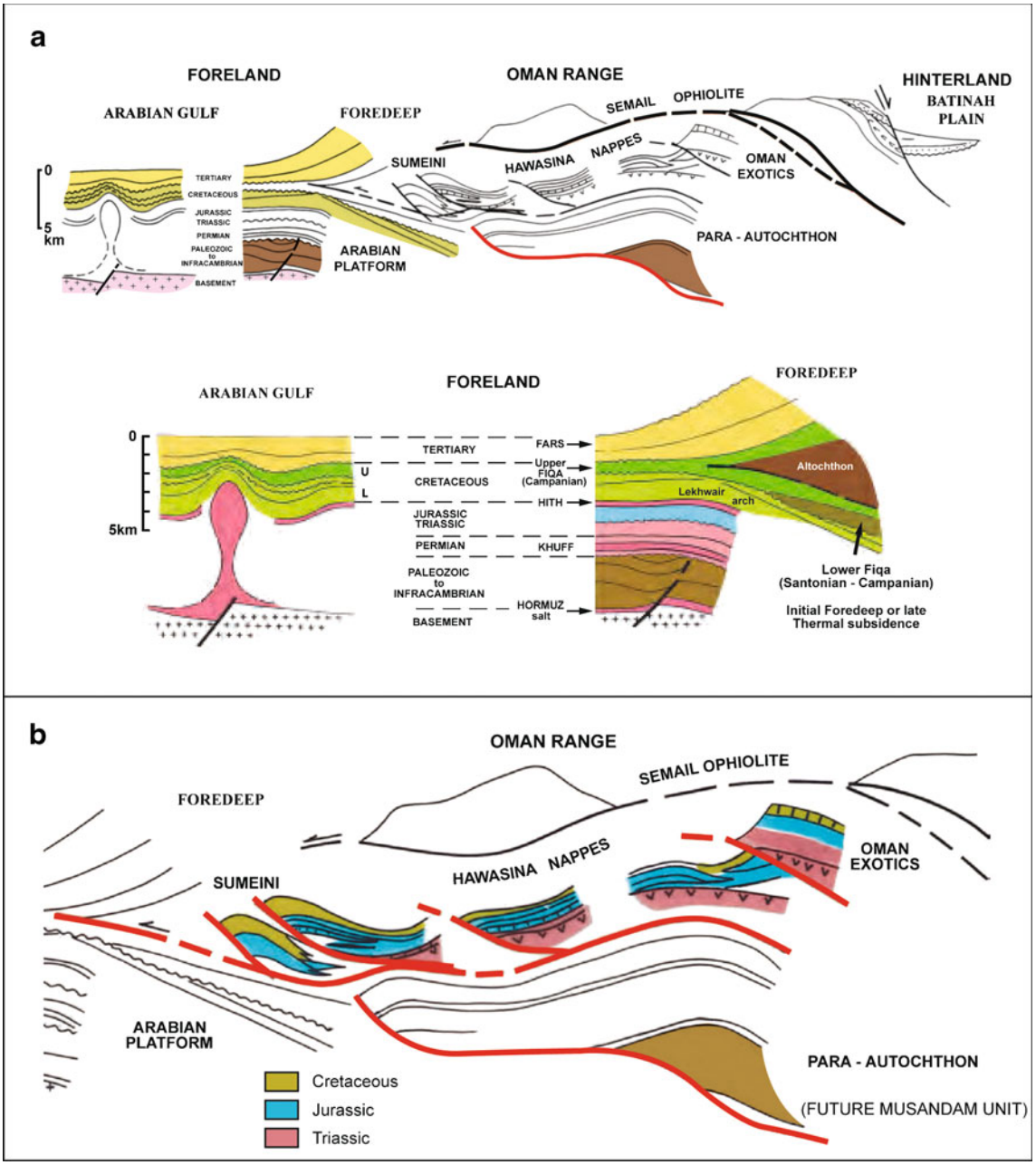

Fig. 3 Sketch outlining the main tectonic and lithostratigraphic units of the Northern Emirates. **a** Relationship between the autochtonous foreland of the Arabian plate and the para autochtonous units of the Munsandam units. Note the pre-existing Hormuz salt diapir and the triangle zone at the front of the Munsandam units. **b** Relationship between the allochtonous slope and basin units (Sumeini and Hawasina) and the para autochtonous Munsandam group, below the ophiolitic bodies. Field work and diagenetic studies were focused on the Musandam Platform carbonates (parautochthonous platform unit), with very limited sampling along the sole thrust of the Hawasina–Sumeini allochthon. Both the autochthonous Arabian foreland and the Hawasina–Sumeini allochthon, which are tectonically located below and above the Musandam Platform unit, respectively, have also been investigated by means of subsurface data, and integrated in the regional structural section D4 used as the main input data for the modelling

(Fig. 2). These breccias likely account for another, major episode of uplift and erosion in this portion of the margin, which predates the onset of thrusting and must therefore be slightly older than the forebulge development recorded farther to the west. Although these breccias are poorly dated, they rework numerous carbonate boulders and clasts, the youngest reported ages for these reworked lithologies being Aptian in age. Because of the strong erosion (locally down to the Permian), they could relate to the local inversion of pre-existing high-angle faults and grabens of the former passive margin, during an early episode of coupling between the Arabian craton and the plate boundary. Similar foreland

inversions have been documented elsewhere in the Arabian plate, i.e. in the vicinity of the Bagdad High in Iraq, where they can be dated as Cenomanian in age.

Apart of this (these) early episode (s) of emersion, the carbonate units of the former Arabian passive margin record two major, well-documented episodes of shortening associated with thin-skinned tectonics. The first one was active during the Late Cretaceous, when the Hawasina–Sumeini accretionary wedge propagated over 80 km on top of the underthrust Arabian carbonate margin. The second episode operated during the Neogene, accounting for the out-of-sequence thrust emplacement of the Musandam Platform units along the Hagab Thrust, the later which accommodated about 15 km of shortening, and the stacking of deeper duplexes (Ricateau and Riché 1980; Searle et al. 1983; Searle 1985, 1988a, b; Hanna 1986, 1990; Tarapoanca et al. 2010 this volume).

The tectonic regime remains less constrained for the Paleogene. In the west, continuous sedimentation was recorded in the foredeep basin, with the deposition of the dominantly shaly Pabdeh Formation, whereas in the offshore Fujairah in the east, thick Paleogene clastics resulted from the continuous unroofing of the Semail Ophiolite. Various, still debated geodynamic hypotheses have been proposed to account for the Paleogene evolutionary stages of the Northern Emirates, with either (1) continuous compression in the foothills in the west and post-orogenic collapse in the east (Boote et al. 1990), and/or (2) progressive unflexing in the west, coeval with a slab detachment. Both schemes would result in a progressive uplift and unroofing of the former Aruma foredeep. This reversal in the vertical motion of the foreland is well recorded in the Iranian offshore, west of the Hormuz Strait, and onshore in the Eastern Fars Mountains, by the truncation of the top-Pabdeh strata by a major unconformity at the base of the Neogene Fars series (Jahani et al. 2009). Additional evidence of post Cretaceous unflexing is evidenced in the Central Oman foreland by the west-dipping attitude of the autochthonous Arabian platform and basement beneath the Hawasina allochthon (Boote et al. 1990). A summital truncation of the top-Pabdeh series beneath the unconformable Neogene Fars series is also observed in the Ras-Al-Kaimah foothills along the transect D4, despite this part of the former Aruma-Pabdeh foredeep basin is now involved in the frontal triangle zone (Tarapoanca et al. 2010 this volume).

Petrographic studies aiming at Paleo-fluids characterisation

Carbonates are very sensitive to any change in the composition of formation waters. Despite the fact that paleo-environment and early diagenetic episodes have a strong impact on the development and preservation of the subsequent reservoir quality, carbonate reservoirs remain continuously exposed to further diagenetic episodes during deep burial or when they are affected by pressure-solution (stylolites) and fracturing. Classic petrographic studies of thin-sections are commonly combined with micro-thermometer, chemical analyses of fluid inclusions as well as stable isotope studies on neo-formed crystals developing in the rock matrix or in cemented fractures during the various stages of evolution. This combination of analytical techniques allows deriving a paragenetic sequence documenting the succession of mineralogical changes related to former paleo-fluids which once occurred in the porous medium. Cross-cutting relationships between cemented fractures and stylolites, coupled with paleo-stress studies, can also be helpful in constraining a relative timing between these successive paleo-fluid records and the local tectonic scenario (Swennen et al. 2000; Van Geet et al. 2002; Benchilla et al. 2003; Ferket et al. 2003, 2004; Vandeginste et al. 2005; Breesch et al. 2007; Lacombe et al. 2009; Vilasi et al. 2009).

A large amount of petrographic and diagenetic information have been derived from the study of rock samples collected in the Musandam Platform and Sumeini paleo-slope facies in the Dibba Zone. Because most of the analytical results have been published in detail elsewhere (Breesch 2008; Breesch et al. 2006, 2009, 2010a, b), only a summary of the regional carbonate paragenetic sequences is presented and discussed below. The detailed analytical results are presented in Table 1. Some of the diagenetic phases will be discussed in more detail in the "Further evidence for diagenesis at a large scale" section.

Overall paragenetic sequence of the Musandam platform unit and Sumeini slope facies of the Dibba Zone

We did not address any bio-stratigraphic dating in the carbonate series during this study, and major changes have been proposed recently by the BGS in the contours of Jurassic and Lower Cretaceous series in the Musandam unit (Ellison et al. 2009), compared to the older map that we used during our study, many of the outcrops previously mapped as Lower Cretaceous in age being now considered as Jurassic instead (Ellison et al. 2009). In fact, part of these uncertainties are related to the extensive dolomitisation observed in some of the outcrops, making thus difficult to decide whether they ultimately relate to the Jurassic Musandam Group or to the Lower Cretaceous Thamama Group. No matter they are Jurassic or Lower Cretaceous, our dolomitised samples were taken from outcrops, not wells, and were all located close to the top of the platform series.

Table 1 Synthesis of the diagenetic event petrographic and fluid inclusions properties (modified from Breesch 2008; Breesch et al. 2010a, b)

Paragenetic sequence	Location	Structural texture	Host-rock Fm.	Microscopic texture	Composition	CL characteristics	Fluid inclusions (°C)	
							Th	Tfr
Pre-BPS								
Synsedimentary dolomite	WBM	Breccia fragments and matrix	Musandam 2 and 3 Fm.	Planar-S	Non-ferroan dolo	Orange to pink zoned red–yellow		
Host-rock dolomite	WS	Host-rock dolomitisation	Musandam 1 Fm.	Xenotopic dolomudstone-cloudy idiotopic-S	Non-ferroan dolo	Orange to red with bright red overgrowths		
Irregular grey calcite veins	JG	Stockwork veins, matrix of synsedimentary breccias	Mayhah Fm.	Elongated blocky to fibrous	Ferroan Cc	Dull yellow		
Grey calcite cement	Khatt	Thin fractures and moulds of gastropods and corals	Thamama Group	Blocky to elongated blocky	Non-ferroan Cc	Dull orange with sector zonation		
Hanging wall veins:	WG		Ghalilah Fm.					
H1 orange to brown calcite veins		Fracture-shaped veins		Brown twinned elongated blocky	Ferroan cc	Dull brown and yellow luminescent zones		
H2 grey calcite veins		Fracture-shaped veins		Blocky crystals with dense mechanical twinning	Non-ferroan cc	Yellow to dull		
H3 white-yellow calcite veins		Horsetail-shaped veins with several veinlets		Elongated crystals spanning veinlets	Ferroan cc	Dark brown to non luminescent	(131 to 175)	−50 to −33
F1 white calcite footwall veins	WG	En echelon arrays of veinlets	Thamama Group	Blocky to fibrous crystals	Non-ferroan cc	Dark dull		
Calcite precipitates	WBM	Geodes and nodules	Musandam 2 and 3 Fm.	Radiaxial fibrous	Non-ferroan cc	Complex zonations		
Post-BPS to pre-TS								
Brown calcite veins	Khatt	Breccia veins with floating host-rock fragments	Thamama Group	Rhombohedric to baroque crystals+dark brown rim	Slightly ferroan cc	Very fine bright- non zonations		
				With sweeping extinction	Dolomite rim	Non luminescent		
Yellow brown dolomite-calcite veins	WB	Fracture-shaped veins	Ghalilah Fm.	Xenotopic-A	Ferroan dolo- cc	Dark brown with yellow patches	(75 to 146)	−72 to −55
White-brown calcite-dolomite veins	WS	Fracture-shaped veins and moulds and vugs	Musandam 1 Fm.	Cloudy coarse saddle dolomite, sweeping extinction	Ferroan dolo	Non luminescent		
				Blocky calcite with mechanical twins	Non-ferroan cc	Dull orange with luminescent twin planes	124 to 174	−70 to −55
White calcite veins with quartz	JG	Conjugate system of en echelon vein arrays	Ausaq Fm.	Elongated blocky to blocky	Ferroan cc	Dull	115 to 226	−40.2 to −34.1
			Slump zones of Mayhah Fm.	Brown-coloured, turbid with curved thick twins	Quartz	Quartz: non	122 to 209	−41.2 to −35.7
White calcite cement	Khatt	Centre of brown veins or large fractures in centre fault zone	Thamama Group	Blocky to sparry mm-sized crystals with abundant mechanical twins and clear cleavage planes	Non-ferroan cc	Dull brown		
White calcite veins	WB	Fracture-shaped veins	Ghalilah Fm.	Elongated blocky+fine-crystalline blocky crystals	Ferroan cc	Dull orange finely zoned to sector zoned	(75 to 165)	−59 to −56
F2 white calcite footwall veins	WG	Fracture-shaped veins	Thamama Group	Fine crystalline to large deformed crystal texture	Non-ferroan cc	Dull to non luminescent		
Post TS syntectonic								
fibrous brown calcite veins	JG	Breccia matrix cement, slickensides, stockwork veins Fracture-shaped veins	Fault zone Mayhah/ Shamal Chert Fm.	Elongated to fibrous+dark brown blocky	Ferroan cc	Bright orange		
F3 white calcite footwall veins	WG	Within tectonic stylolites	Thamama Group	Large blocky crystals	Non-ferroan cc	Dull to non luminescent		
F5 white calcite footwall veins	WG	En echelon and fracture-shaped veins	Thamama Group	Border: veinlets with elongated blocky crystals	Non-ferroan cc	Dull with zonations and yellow spots	81 to 166	−95 to −68
				Centre: fine crystalline brecciated calcite				
Stockwork veins	WG	Stockwork microfractures	Thamama Group	Calcite with abundant mechanical twins	Non-ferroan cc	Not luminescent		

Table 1 (continued)

Paragenetic sequence	Location	Structural texture	Host-rock Fm.	Microscopic texture	Composition	CL characteristics	Fluid inclusions (°C)	
							Th	Tfr
Pre-BPS								
Dolomite recrystallisation and cement	WBM	Thin border around breccia clasts, in pores, as clusters	Musandam 2 and 3 Fm.	Non-planar elongated crystals	Non-ferroan dolo	(1) Purple to non and (2) pink to yellow phase		
Quartz cement and silicification	WBM	Interbreccia fragment pores	Musandam 2 and 3 Fm.	Fine-crystalline	Quartz	Non luminescent	100 to 250	−35 to −32
Host-rock dolomite	WB	Host-rock dolomitisation	Milaha Fm.	Fine-crystalline idiotopic-S	Non-ferroan dolo	Dark red		
Pink dolomite cement	WB	Cavities and parallel fractures	Milaha Fm.	Xenotopic-C saddle dolo with undulose extinction	Non-ferroan dolo	Dark red cores- bright non zoned rims	139 to 193	−75 to −63
Dolomite recrystallisation and cement	WS	In dolomite host rocks, vug fillings	Musandam 1 Fm.	Euhedral to slightly baroque	Non-ferroan dolo	Red core and red zoned rim- red overgrowths		
Post deformation								
Yellow calcite veins	JG	Long continuous fracture-shaped veins	Mayhah and Ausaq Fm.	Blocky to elongated blocky	Ferroan cc	Bright orange with yellow spots	(155 to 286)	−41.3 to −34.1
Speleothems	WBM	Stalagmites	Musandam 2 and 3 Fm.	Alternating radiaxial fibrous and blocky crystals	Non-ferroan cc	Non luminescent-blotchy dull orange	60	−43 to −39.5
Black calcite cement	Khatt	Dispersed in host rocks and in remaining pores in fractures	Thamama Group	Fine-crystalline, slightly rounded, few twins	Non-ferroan cc	Large-scale bright-non luminescent zoning		−46 to −39
White calcite cement	WB	Cavities and parallel fractures	Milaha Fm.	Large sparry crystals	Non-ferroan cc	Non lum border and large orange zonations		
White calcite cement	WS	Vugs and moulds	Musandam 1 Fm.	Blocky	Non-ferroan cc	Thinly zoned bright phase- non lum phase		

Paragenetic sequence	Fluid inclusions (°C)					Stable isotopes	
	Tfm (min.)	Tm ice	Thh	Fluid system	Salinity (wt%)	δ18O (δ ΠΔB)	δ13X (δ ΠΔB)
Pre-BPS							
Synsedimentary dolomite						−9.8 to −2.7	−8.5 to −0.6
Host-rock dolomite						−6.8 to −1.8	−2.3 to −0.2
Irregular grey calcite veins						−6.6 to −2.3	+0.9 to +3.3
Grey calcite cement						−6.0 to −3.2	+2.1 to +2.7
Hanging wall veins:						−8.0 to −7.0	−1.5 to 0.0
H1 orange to brown calcite veins							
H2 grey calcite veins							
H3 white-yellow calcite veins		−3.6 to −1.7			2.9 to 5.9		
F1 white calcite footwall veins						−4.0 to −3.5	+1.4 to +1.7
Calcite precipitates						−8.2 to −3.8	−11.0 to −3.8
Post-BPS to pre-TS							
Brown calcite veins						−9.6 to −7.9	−6.6 to −3.5
Yellow brown dolomite-calcite veins	−45	−27.8 to −9.5	−24 to −22	H_2O–NaCl–$CaCl_2$		−12.7 to −5.5	−3.9 to −0.9
White-brown calcite-dolomite veins						−8.9 to −5.2	−1.8 to 0.3
	−31.5 to −17.7	−21.1 to −14.5		H_2O–NaCl–(KCl)	18.22 to 23.11	−6.2 to −3.3	−2.2 to −0.9
White calcite veins with quartz	−19.4	−1.2 to −0.7		H_2O–NaCl	1.23 to 2.07	−8.3 to −2.9	+2.0 to +3.3

Table 1 (continued)

Paragenetic sequence	Fluid inclusions (°C)					Stable	isotopes
Pre-BPS	Tfm (min.)	Tm ice	Thh	Fluid system	Salinity (wt%)	δ18O (δ ΠΔB)	δ13X (δ ΠΔB)
	−5	−1.6 to −1.0			1.74 to 2.74		
White calcite cement						−6.7 to +0.1	−0.1 to +2.6
White calcite veins		−4.1 to −3.3			5.41 to 6.59	−14 to −12	−2.5 to −0.3
F2 white calcite footwall veins						−3.8	+1.5
Post TS syntectonic							
fibrous brown calcite veins						−12.3 to −5.9	−1.1 to +1.8
F3 white calcite footwall veins						−3.6 to −2.5	+0.9 to +1.7
F5 white calcite footwall veins	−53 to −44	−28 to −18.3		H_2O–NaCl–$CaCl_2$	>20	−6.7 to −4.0	+1.5 to +1.8
Stockwork veins						−6.1 to −3.8	+1.4 to +1.9
Dolomite recrystallisation and cement						−9.9 to −7.8	−8.5 to −6.7
Quartz cement and silicification						18.46 to 20.60	‰ SMOW
Host-rock dolomite						−11.7 to −8.9	+1.0 to +1.4
Pink dolomite cement	−41	−23 to −7.4		H_2O–NaCl–$CaCl_2$		−11.5 to −10.0	+0.5 to +1.0
Dolomite recrystallisation and cement						−9.9 to −6.3	−1.2 to −0.3
Post deformation							
Yellow calcite veins	−25.9	−2.7 to −1.1		H_2O–NaCl	1.91 to 4.49	−5.3 to −4.4	+0.9 to +2.4
Speleothems		−1.6 to −0.1			0.18 to 2.74	−9.9 to −5.6	−6.6 to −3.9
Black calcite cement		−0.6 to 0			0 to 1.05	−11.6 to −10.4	−6.6 to −5.7
White calcite cement						−4.7 to −3.6	+0.3 to +0.8
White calcite cement						−12.7 to −7.1	−9.4 to −1.9

JG Jebel Gharaf, *WBM* Wadi Batah Mahani, *WG* Wadi Ghalilah, *WS* Wadi Sha'am, *WB* Wadi Bih, *Th* homogenisation temperature, *Tfr* freezing temperature, *Tfm* first melting temperature, *Thh* Hydrohalite melting temperature, *Tmice* last ice melting temperature

The regional paragenetic sequence could be differentiated into different time periods based on the occurrence of different generations of stylolites. As summarised in Fig. 4, burial stylolites developed at two different times in the Musandam Platform unit, first during the episodes of sedimentary burial associated with the development of the passive margin, and then during the subsequent episodes of tectonic burial beneath the Sumeini–Hawasina allochthon. However, the tectonic stylolites in the Musandam platform carbonates are much younger than the ones in the Sumeini paleo-slope carbonates in the Dibba Zone. LPS Stylolithes in Sumeini units had a NE–SW strike, perpendicular to NW–SE Late Cretaceous compression while the LPS in Musandam had NS strikes (Wadi Ghalilah) perpendicular to EW Cenozoic compression. Based on the occurrence of these stylolites, the regional carbonate paragenesis can be subdivided into four time periods with their typical vein associations (Figs. 4 and 5, Table 1) could be established. In summary, marine (synsedimentary) to burial, syntectonic and post-deformation veins can be distinguished. Other diagenetic features comprise dolomites, which can be divided in penecontemporaneous (related to depositional environment and early burial) and syntectonic dolomites. The latter are of importance for the fluid system reconstruction since extra-formation fluids are often invoked for their formation. These dolomites will be described in more detail in the next section.

Two phases of emersion and karstification are recorded in the carbonates of the Musandam Platform unit, the first one during the Mid-Cretaceous shortly after deposition, the second one corresponding to late telogenetic exhumation (Figs. 4 and 5). At this stage, two distinct hypotheses can be proposed for the Mid-Cretaceous emersion episode. The first hypothesis relates to the development of the forebulge, during the Turonian–Campanian, at the onset of tectonic loading operating on the distal portion of the

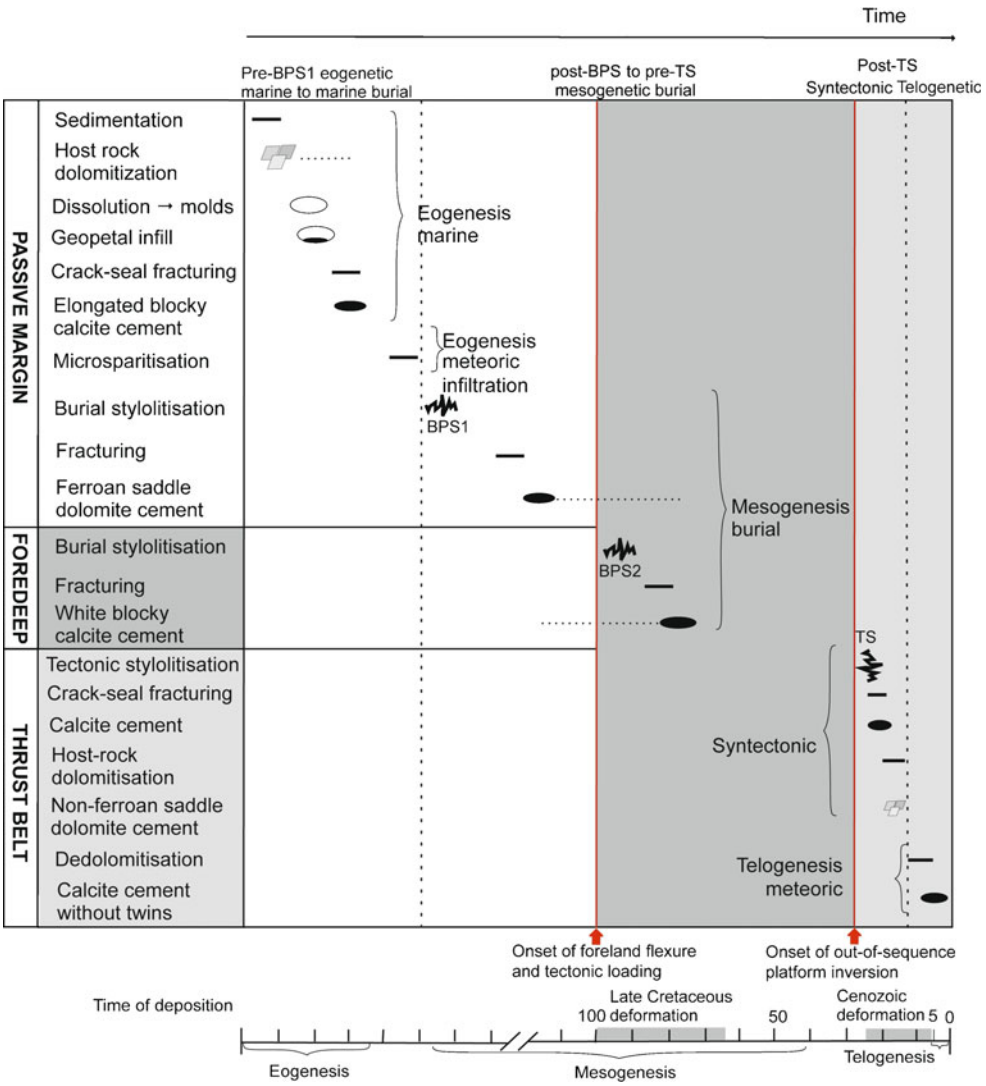

Fig. 4 Overall paragenetic sequence of the Northern Emirates carbonates (Musandam and Sumeini outcrops), outlining the succession of emersion, cementation, pressure-solution and fracturing events, grouped following the main geodynamic stages: passive margin evolution, foreland basin compression stage and main thrusting episode (from Breesch 2008; Breesch et al. 2009). This sequence is summarised in Table 1

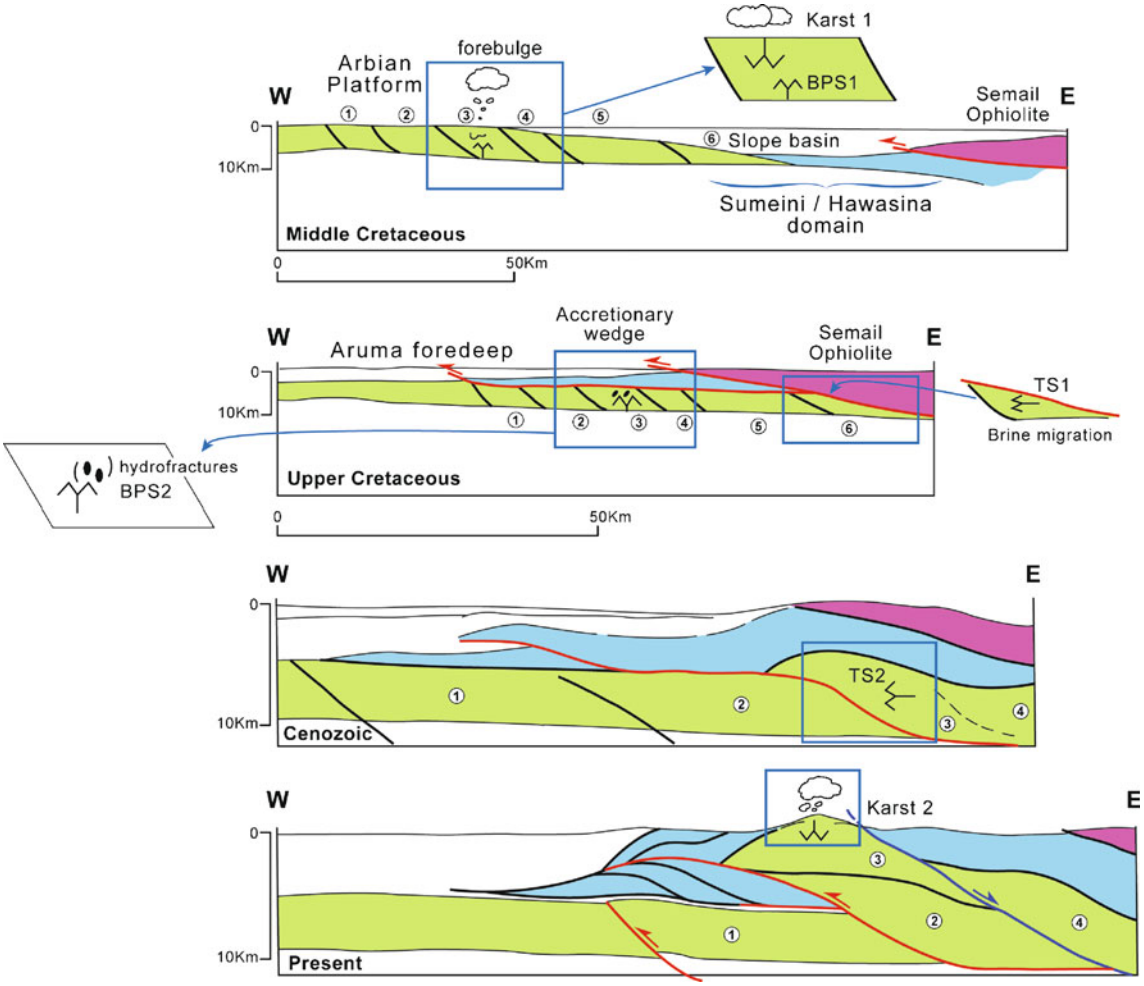

Fig. 5 Evolutionary sketch of the Musandam-Dibba section and its links with diagenetic evolution (after Breesch et al. 2010a). *BPS* bed-parallel stylolithe, *TS* Tectonic stylolithes, *LPS* layer parallel shortening. *1–3* Units of the Musandam platform, *4* Sumeini slope; *5* Pieces of Hawasina Basin; *6*: Ophiolite

Arabian lithosphere. Alternatively, the emersion could be related to an earlier, Cenomanian episode of foreland inversion, when a strong tectonic coupling occurred between the converging Arabian and Tethyan plates. The latter hypothesis is locally supported by the occurrence of a major erosional unroofing of the southeastern part of the Musandam Platform near its contact with the Dibba Zone. There, the post-Aptian polymictic breccias of the Ausaq Formation, deposited in the footwall of the Hawasina–Sumeini allochthon, rest unconformably on top of Lower Cretaceous, Jurassic, Triassic and even Permian rocks (Ellison et al. 2006, 2009; Phillips et al. 2006), thus recording a pre-obduction episode of foreland inversion and erosional unroofing. The diagenetic products of these emersion phases will also be discussed in more detail in the next section.

Based on the results from the case studies in the Musandam Platform unit, a large-scale fluid system is invoked with migration of hot brines with an H_2O–NaCl–$CaCl_2$ composition along Cenozoic reverse faults (Breesch 2008; Breesch et al. 2010b). These brines were sourced via the Hagab Thrust from deeper formations or even from the basal decollement level. They do only infiltrate in the footwall blocks along the reverse faults resulting in compartmentalisation (Breesch 2008; Breesch et al. 2009).

When compared with similar studies on foreland fold-and-thrust belts in other regions, the timing of the various vein and stylolite associations with respect to pre-orogenic, synflexural and then syn-kinematic periods is in general comparable. Only the veins which are interpreted as crack-seal veins based on their petrographic characteristics (Table 1), postdate the tectonic stylolites in the Musandam Platform in contrast with classic fold-and-thrust belts. The lack of mesogenetic hydraulic fractures predating tectonic stylolites in the Musandam Platform unit is likely due to its dominantly carbonate lithology, which prevented overpressures to devel-

op before an efficient seal made up by the Sumeini–Hawasina allochthon was tectonically emplaced on top of the platform. Assuming that the tectonic stylolites (LPS) developed at the onset of the Cenozoic compression, when the Munsandam Platform was still in the footwall of the active thrust system, subsequent hydraulic and crack-seal veins are best interpreted as local features only, caused by fault activity associated with tectonic uplift of the Musandam Platform unit during the Hagab Thrust emplacement.

Despite careful surveys, no bitumen or oil seeps have ever been described in surface outcrops of the Musandam Platform. However, the existence of a mature petroleum system in the region is confirmed by the occurrence of green fluorescent fluid inclusions in calcite veins in the Musandam limestones. Therefore, sub-thrust platform and slope carbonates have to be considered as hosting potential hydrocarbon reservoirs as soon as the petrophysical characteristics are favourable. Particularly, dolomite recrystallisation at the platform border is a possible process to create poorly connected reservoirs (see next section). When the migration of hot brines along the Cenozoic reverse fault would be combined with petroleum migration, the footwall compartments also could act as potential reservoirs, sealed by the fault.

Further evidence for diagenesis at a large scale

In this section, the diagenetic products and processes which provide evidence for the existence of an open fluid system will be discussed in more detail (see also table 1).

Hot dolomitizing fluid

Samples collected in Wadi Batha Mahani are located very close to the tectonic contact separating the Musandam platform from the Hawasina–Sumeini units of the Dibba Zone. However, seismic imagery (profile D4 and other industry profiles recorded in the same area), demonstrate that a wide Mesozoic sedimentary unit still extends in the subsurface beneath the allochthon. This makes it difficult to constrain the former paleogeography, especially whether the transition between the carbonate platform and the slope occurred at the current location of the Dibba Fault zone, or was instead located farther east, within the still currently underthrust footwall domain. Either way, whether this part of the Musandam Platform unit was located close to the slope, or was instead underlain by a high-angle fault inherited from the former rift, it is dominated by the presence of patchy dolomite breccia (Fig. 6; Breesch et al. 2010a, b).

Two main events of dolomite formation were identified along the southern border of the Late Jurassic Musandam carbonate platform.(see Table 1)

The first dolomitisation phase (type 1) was restricted to specific stratigraphic layers in Jurassic platform limestones that were subsequently brecciated by mass flow and collapse processes on the platform margin. These dolomites are planar-s, have crystal sizes ranging from 5 to 25 μm and exhibit an orange to pink and sometimes zoned red–yellow luminescence. This dolomite phase was formed shortly after deposition by fluids of marine or slightly modified marine composition (Breesch et al. 2006, 2010a). The second dolomite phase (type 2) mainly affected dolomite type 1 breccias by recrystallisation, dolomite cementation and replacement. Type 2 dolomites are planar-e and non-planar-c, with crystal sizes between 20 and 70 μm. They have more elongated forms with purple luminescent to non luminescent cores overgrown by pink to yellow luminescent rims. Stable isotope analyses show a covariant trend between $\delta^{18}O$ and $\delta^{13}C$ from marine (−4.2 to −1.8 and +0.8 to +2.1‰ VPDB, respectively) towards depleted values (−10.2‰ and −8.9‰ VPDB, respectively; Breesch et al. 2006, 2010a). This depletion is explained by recrystallisation during type 2 dolomitisation and it is interpreted in terms of high temperatures during precipitation and the incorporation of light carbon as hydrocarbons matured. Dolomite type 2 formation is thought to be the result of tectonically induced fluid flow which supplied hot magnesium-rich fluids (Breesch et al. 2006, 2010a). Due to the fact that the timing of this phase is difficult to

Fig. 6 Outcrop outlining the contours of a relict Musandam limestone in pervasively dolomitised breccias (tree and geologist for scale)

constrain, we are currently considering three hypotheses, the first and last ones being the most likely:

1. Vertical expulsion of hot basinal fluids could have occurred already during the Cenomanian, when foreland inversion initiated in the vicinity of high-angle faults in various parts of the Arabian plate as well as at the southeastern margin of the Musandam Platform. This hypothesis could be supported by the occurrence of reworked dolomitic pebbles in the younger Cretaceous breccias which rest unconformably on top of various Permian, Triassic, Jurassic and Lower Cretaceous carbonate series.
2. Tectonically induced fluid flow that takes place along the sole thrust of the Hawasina–Sumeini allochthon during its Late Cretaceous thrust emplacement over the Musandam Platform. Volcaniclastic and basaltic rocks of the Hawasina Complex and the Oman–UAE ophiolites are a possible magmatic source for magnesium in this case. In support of this hypothesis, hydraulic fractures and shear bands have effectively been evidenced in the Ausaq breccias below the sole thrust of the Hawasina–Sumeini allochthon. As described below in paragraph 3.3, cements in these breccias host fluid inclusions that are also characterised by high trapping temperatures and salinities (Vilasi 2003). However, these fluids and coeval deformation features appear to be restricted, at outcrop scale, to a very narrow zone, extending only for a few metres beneath the basal décollement. They are therefore unlikely to have impacted the underlying platform carbonates at a larger extent.
3. Hot post-evaporative brines migrated along the out-of-sequence Hagab thrust, which acted as a fluid conduit during the Cenozoic orogeny, collecting fluids mobilised by the tectonic loading and flexing of the margin.

Cold meteoric water

Two episodes of karstification have been evidenced in the Musandam Platform unit.

1. The first pre-Cenomanian phase of meteoric water infiltration resulting in karstification in the Musandam Formation is characterised by dissolution with subsequent geopetal infill and microsparitisation of the shallow marine deposits of the Musandam Formations is observed. Nodular limestones and hardground surfaces with soil-related nodules are present. Vugs filled with sediments are found in most limestones. The Jurassic–Cretaceous limestones were also partially to completely microsparitised. Limestone dissolution and precipitation of radiaxial fibrous calcite cement within geodes and nodules has been observed in The Musandam Formations in Wadi Batha Mahani (Table 1). These non-ferroan calcite precipitates display complex CL zonations and are characterised by negative values for $\delta^{18}O$ and $\delta^{13}C$ (respectively between −8‰ and −5‰ and between −6.5‰ and −4‰; Table 1). Sedimentary infill in some of these cavities was subsequently silicified (Fig. 7a, b; Table 1).
2. The second phase of karst development is a telogenetic one. Post-tectonic calcite cement, characterised by blocky textures and the absence of mechanical calcite twins, is present in dissolution-related features such as moulds and vugs and in irregular seams in the host rocks. Apart from this, also caves and karst cavities formed with calcite precipitation inside (Fig. 7c,d; Table 1). The stable isotope signatures of these post-tectonic calcites are very depleted for both $\delta^{18}O$ and $\delta^{13}C$ with values down to −13‰ for $\delta^{18}O$ and −9‰ for $\delta^{13}C$ (Table 1).

Hydraulic fracturing and cemented veins near the sole thrust of the Hawasina allochthon

Cemented veins were also studied and collected in the footwall of the Hawasina allochthon in the Dibba Zone, in post-Aptian breccias of the Ausaq Formation, which unconformably overlay older series along the southeastern border of Musandam unit (Ellison et al. 2006, 2009; Phillips et al. 2006).

The conglomerates of the Ausaq Formation interdigitate here with the slumped mudstones of the Mayah Formation. Several vein generations are present and can be grouped into early marine to marine burial, burial, syntectonic Late Cretaceous, and post-deformation periods, based on their relation with the burial and tectonic stylolite generations and their petrographic and geochemical characteristics. One vein generation supplies evidence for deformation in a shear zone (Fig. 8).

In the first vein generation, primary inclusions have low final melting temperature (Tfm) traducing a global high salinity of 25 wt.% equ. NaCl. The initial melting temperature (Tmi) are lowered until −45°C traducing the presence of $CaCl_2$. The correlation between Tfm and Tmi (Fig. 9, bottom c) indicate a variability of the calcium content instead of the NaCl content. Homogenisation temperature range from 160°C to 180°C. These fluids should come from deep levels and have probably dissolved evaporitic layer before they circulated along fractures.

Secondary inclusions present higher temperatures and wider range values from 180°C to 280°C. They can be divided into 4 classes of temperature, presenting the following average of homogenisation temperature: 190°C (F1); 215°C (F2); 250°C (F3); >270°C (F4). The four families of homogenisation temperature, entrapped as secondary fluid inclusions, indicate a paleo-fluid circulation after the mineralisation of the second vein generation. Re-

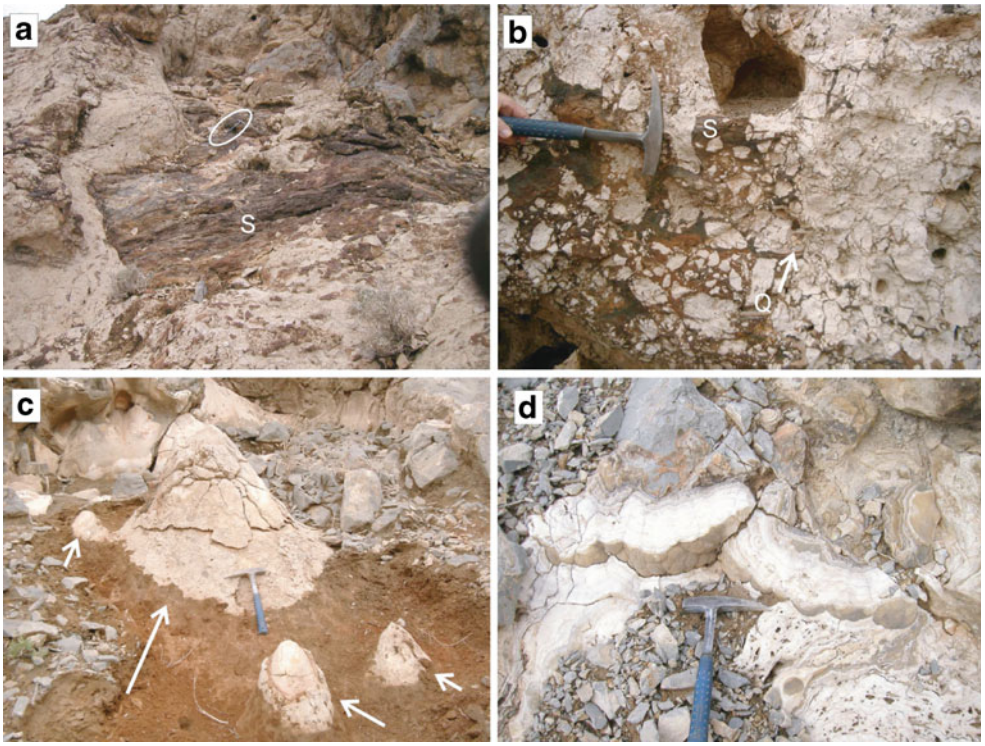

Fig. 7 Outcrop pictures from the Musandam unit evidencing various meteoric karst records. **a** and **b** Karst phase 1: dissolution cavities with silicified sediment infill (*S*) and quartz (*Q*) cement. **c** and **d** Karst phase 2: vertical directed calcite stalagmites (*arrows*) and botryoidal crust-forming calcite speleothem in dissolution cavities. Hammer (32 cm) for scale

opening process has created these intra-granular micro-fractures in the second vein generation

The maximum burial of the Musandam carbonates and Ausaq breccias is hardly constrained by the regional geological data, due to the present attitude of the erosional surface. Isolated erosional remnants of Hawasina material have been found locally at the top of the Musandam Platform. Seemingly, the Hawasina series are cropping out in the core of the Hagil tectonic window (Fig. 2), in the footwall of the Hagab Thrust, thus implying that the Musandam Platform unit was once entirely overlain by the allochthon. However, as demonstrated by the Apatite Fission Track ages obtained from plagiogranites intruding the Semail Ophiolite (Naville et al. 2010, this volume; Tarapoanca et al. 2010, this volume), the later was already deeply eroded prior to final emplacement of the allochthon on top of the Arabian foreland during the Late Cretaceous. Assuming a geothermal gradient of 30°C/km, it sounds difficult to account for temperatures in excess of 200°C at the base of the allochthon (i.e. at the top of the Musandam Platform carbonates and Ausaq breccias), without assuming that these temperatures indeed reflect the advection of hot fluids coming from deeper levels.

Fig. 8 Cemented hydraulic fractures in the Upper Cretaceous breccias of the Ausaq Formation, resting unconformably above various stratigraphic horizons of the Musandam unit ranging from Permian to Lower Cretaceous. These breccias are located in the footwall of the Hawasina–Sumeini allochthon

Ceres fluid flow modelling along profile D4

Principles

Basin modelling aims at reconstructing the time evolution of a sedimentary basin in order to make quantitative predictions of geological phenomena leading to pressure

Fig. 9 Fluid inclusion and microthermometric data from cemented veins of the Ausaq Formation (after Vilasi 2003). *Top* **a** to **d**, blocky calcite minerals with fluid inclusions in the cemented veins. *Red line* shows secondary fluid inclusion type and *green circle* represents primary fluid inclusion type emplacement. *Bottom* microthermometric analyses realised on both types of fluid inclusions in the cemented veins. Diagram **a**, **b**, **c** show homogenisation temperature (Th) for primary fluid inclusions (*blue*) and for secondary fluid inclusions (*red*). Diagram **c** presents first (Tfm) and final melting temperature (Tmi) of primary fluid inclusions

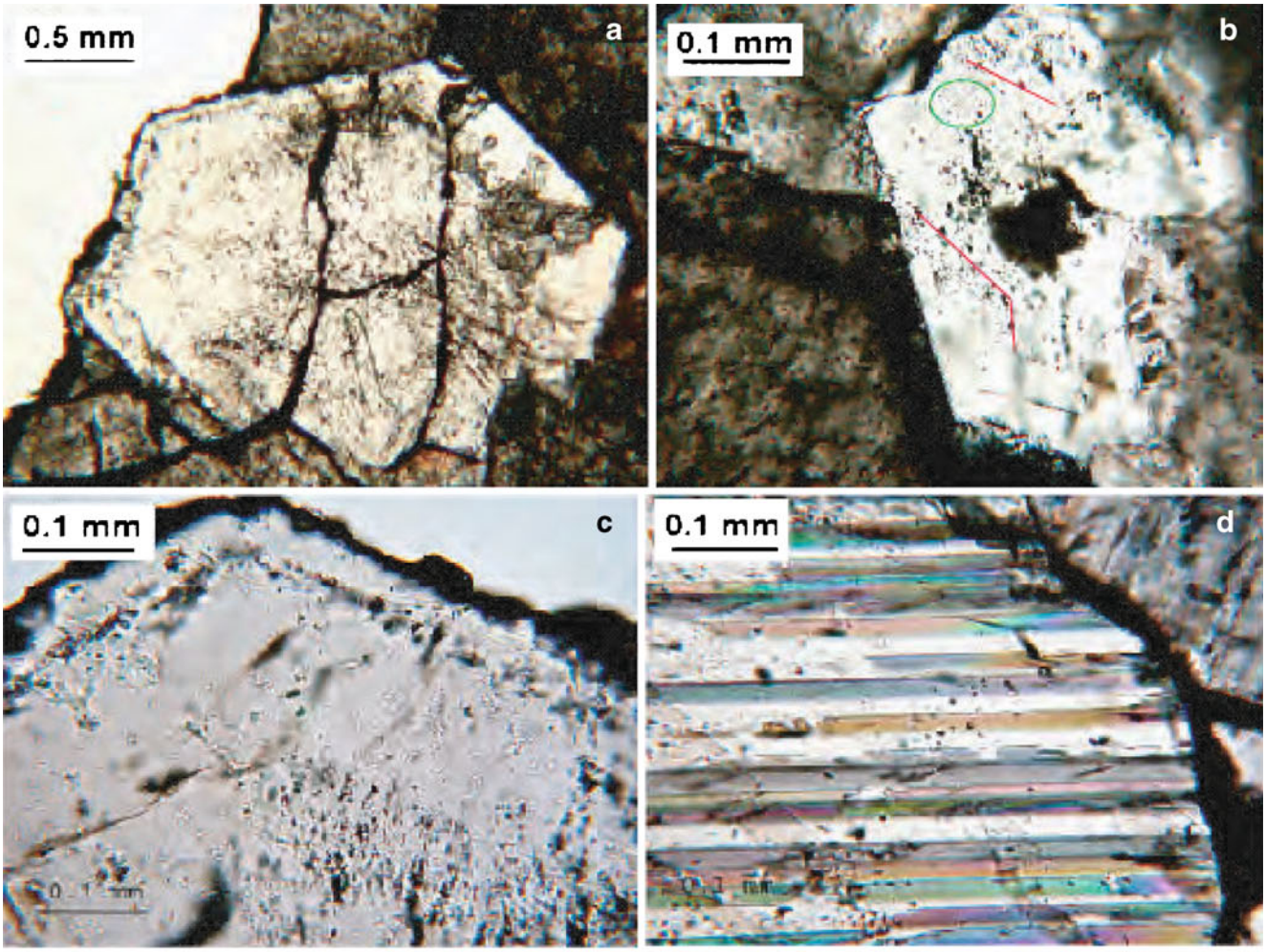
0.5 mm
a
0.1 mm
b
0.1 mm
c
0.1 mm
d

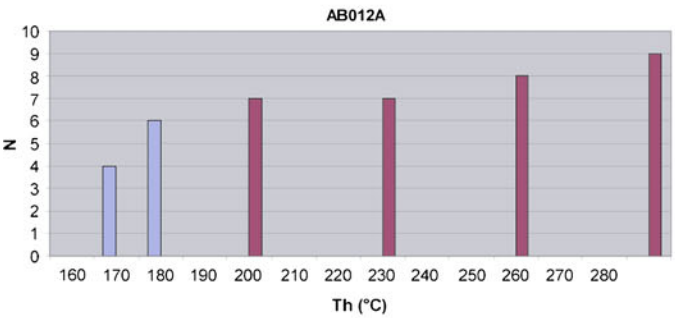
AB012A
N
Th (°C)
160 170 180 190 200 210 220 230 240 250 260 270 280

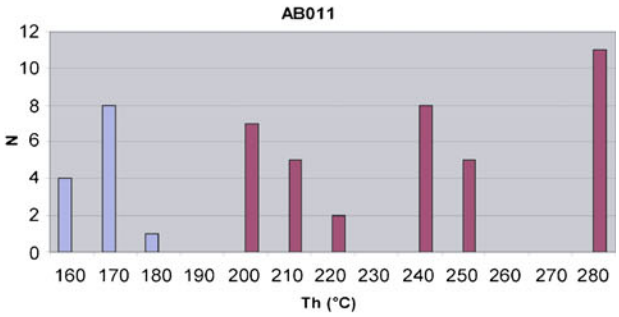
AB011
N
Th (°C)
160 170 180 190 200 210 220 230 240 250 260 270 280

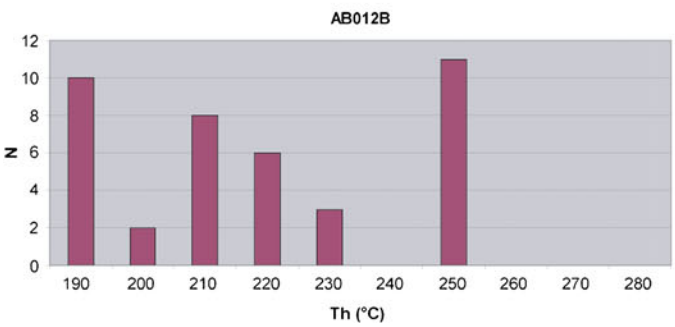
AB012B
N
Th (°C)
190 200 210 220 230 240 250 260 270 280

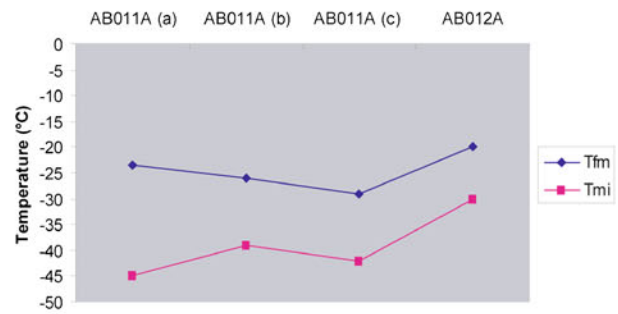
AB011A (a)
AB011A (b)
AB011A (c)
AB012A
Temperature (°C)
Tfm
Tmi

generation and hydrocarbons accumulations. It accounts for porous medium deformation, heat transfer, pore-fluid pressure and flow modelling, hydrocarbon formation and migration (e.g. Schneider et al. 2002).

Two distinct basin modelling tools have been used to better assess the thermal evolution and hydrocarbon potential along the regional transect D4 crossing the Northern Emirates from the Gulf of Oman in the east up to the Arabian Gulf in the west (Figs. 2 and 10): (1) Thrustpack, which proceeds by means of a forward kinematic approach (Sassi and Rudkiewicz 2000), and computes the paleo-temperatures and maturity evolution of the organic matter through time, but cannot handle the evolution of the pore-fluid pressures and the fluid flows (i.e. neither the circulation of compaction waters nor the migration of the hydrocarbons), and (2) Ceres2D (Schneider et al. 2002; Schneider 2003), which proceeds by means of backstripping, and can account for convective heat and fluid transfers in complex structural architecture, thus providing 2D scenarios for fluid circulations (both regional water flow and hydrocarbon migration).

Thrustpack kinematic results, which were used as input data to better constrain intermediate target geometries during subsequent Ceres modelling, are detailed in a companion paper (see Tarapoanca et al. 2010). Only the backstripping, fluid flow and pressure regime reconstructed with Ceres will be discussed here, as they provide a direct, reliable numerical analogue to compare with the fluid–rock interactions documented in the rock samples collected in the field and previously described. Other results of the Ceres modelling, dealing with the thermal evolution and hydrocarbon migration and charge, cannot yet be publicly released.

The eastern part of transect D4 (Figs. 2 and 10) is located in the Dibba Zone, an area where the Hawasina basinal and Sumeini paleo-slope allochthonous units crop out at the surface, north of the Semail Ophiolite. Further west, this transect extends across the deepest parts of the foredeep basin. Although the thrust front is deeply buried in this area, it accounts for a classic triangle zone. There, a foreland-dipping monocline connects westwards to a deep blind thrust. Platform carbonates of the Musandam units are exposed at the surface a few kilometres north of the profile, and have been reached in the subsurface by the Juweizi well (Fig. 2). Deeper platform duplexes are evidenced on seismic profiles, and have been locally proven to be productive (gas-condensate) further south in the Margham and Sajaa fields (Blinton and Wahid 1983; Alsharhan 1989; O'Donnell et al. 1994; Fig. 2).

Thrustpack input data and simplified architecture of the modelled transect

Thrustpack modelling already performed along transect D4 provided a validation of the kinematic scenarios as well as a series of intermediate geometries between the pre-orogenic stages of the former passive margin of the Arabian plate and

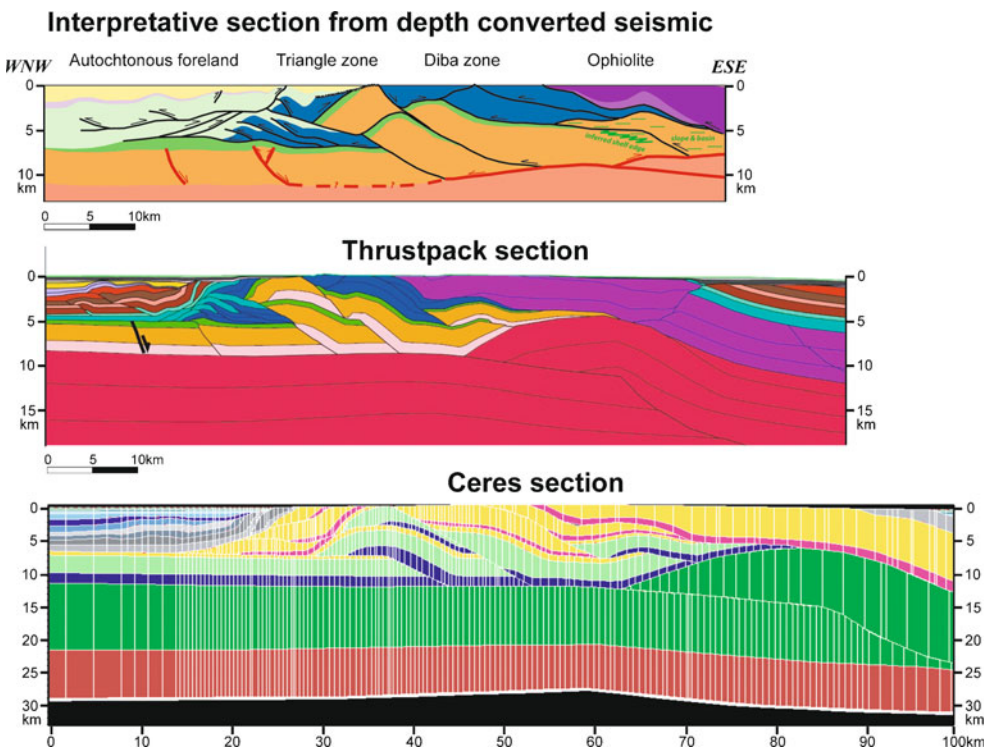

Fig. 10 Present architecture of the regional transect D4. *Top* Structural section derived from the seismic interpretation (see Naville et al. 2010, this volume); *Middle* Simplified Thrustpack section (see Tarapoanca et al. 2010, this volume); *bottom* Simplified Ceres section (*vertical white lines* denote the meshing used for the basin modelling computation in Ceres2D)

the present-day stack of the platform units which characterise the frontal triangle zone (see Tarapoanca et al. 2010).

The Ceres section was directly built from the interpreted Thrustpack scenario of the D4 section (Fig. 10). The main tectonic features of this section document:

1. The occurrence of an early tectonic wedge made up of Hawasina- and Sumeini-type sediments, which has formed at the front of the Semail Ophiolite during its early movements in Santonian/Campanian time;
2. Further stacking and refolding of this early wedge during the emplacement of deeper duplexes made up of fragments of the Arabian platform margin, associated with the refolding/thrusting of former Hawasina and Sumeini units;
3. The late activity of a large high-angle normal or transcurrent fault.

Ceres modelling had to cope with a strong limitation, since due to topological constraints, out-of-sequence thrusting could not be properly simulated. This implied to redraw the frontal part of the section and to simplify the initial cross-cutting relationships between the different sets of faults (Fig. 10). First the frontal parts of the main platform units were closed by extending the forelimb of the anticlines down to the intermediate décollement propagating at the base of foredeep deposits. Secondly, the early stacked Hawasina–Sumeini units were represented as in-sequence thrust units resting on top of deeper platform units, avoiding the main deep thrusts to breach through the basal contact of the far-travelled allochthon. For the same concern, the complex stack of Hawasina–Sumeini units was simplified and replaced by three major thrust sheets only. Similarly, the complex deformed triangle zone containing both forward verging thrusts and backward verging units in the Thrustpack section was slightly modified in the Ceres section. The two main tectonic units in the triangle zone were preserved, but the complex fold-and-thrust structure above the undeformed platform of the lower plate was replaced by a single anticline. These simplifications of the geometry of the section aimed at preventing numerical artefacts, but still preserved the first order characteristics of the present-day architecture (Fig. 10).

Modelling the section with Ceres 2D

Workflow

Three main steps form the milestones of the study: (1) edition of the initial section and data, (2) backward building of the scenario, and (3) forward simulation.

1. The initial section is edited from the former Thrustpack templates. At this stage, the geological attributes are assigned, including the horizons, faults, decollement levels, the section boundaries, and the age and lithology constraints. The various parts or subdomains of the section are then defined as small independent units with a specific meshing.
2. The section is then sequentially restored through time, on the basis of the target intermediate geometries defined by the Thrustpack model, particularly to handle the reconstruction of the missing parts. Backstripping and decompaction of the various sedimentary layers is also accounted for.
3. The forward modelling is the last step, coupling the heat transfer, the fluid pressure and flow distribution, the hydrocarbon formation, solving the mass conservation of solids and fluids, coupled with the Darcy and compaction laws (Schneider et al. 2002; Schneider 2003).

In these complex geometries, faults cut the basin into blocks that naturally define computational subdomains, using the domain decomposition methods (e.g. Faille et al. 1998). For each incremental episode of sedimentation or erosion, the model calculates in each block the porous medium compaction, heat transfer, hydrocarbon formation and migration (Schneider et al. 2002; Schneider 2003). The equations are mass conservations of solid and fluids (water, oil and gas) coupled with Darcy's law and the various compaction laws. The faults have a constant width. Their permeability may evolve with time. The prototype allows using three permeability models for the faults: (1) pervious; (2) impervious or (3) defined with an anisotropic permeability based on the harmonic mean (across fault permeability) or arithmetic mean (along fault permeability) of the properties of the adjacent lithologies. This last option simulates the lateral variability of the fault rocks, implying that the permeability of an individual fault can evolve through time according to its neighbouring lithologies. Permeability can also change with the strain rate.

Ultimately, the faults are considered as inactive when their slip motion is slower than the defined speed limit of 50 m/Ma.

Building of the Ceres scenario through backstripping

Figure 11 summarises the final structural scenario adapted for the modelling. The first episode (not represented here) accounts for the deposition of the pre-rift mega-sequence during the Proterozoic and Paleozoic. It is followed by the Permian–Triassic rifting of the Tethys, with the coeval development of the Arabian carbonate platform and with the deposition of more distal units in the Sumeini paleoslope and Hawasina basinal domains.

Onset of the Tethys closure and obduction of the Semail Ophiolite in the middle/Late Cretaceous were associated with the development of a flexural sequence in the Emirates foreland (Fig. 11a). The obduction of the Semail Ophiolite forced the emplacement of a large pile of Hawasina–Sumeini thrust sheets above the underthrusted Arabian platform domain before the end of the Cretaceous (Fig. 11b).

The Paleogene extension recorded within the Gulf of Oman, associated with a coeval collapse of the Oman Range, is not modelled here. Actually, a major uncertainty still relates to the precise timing of the deformation in areas currently located between the frontal triangle zone and the erosional front of the Semail Ophiolite. For instance, we do not know whether the well-documented Late Cretaceous (Fig. 11a to e) and Neogene (Fig. 11f and g) episodes of shortening were separated or not by a long period of tectonic quiescence. In the first case, Paleogene uplift and erosion could have been controlled by slab detachment and coeval unflexing of the foreland lithosphere, without synchronous tectonic shortening (Tarapoanca et al. 2010 this volume). Alternatively, a continuum of compressional deformation and shortening could have operated over the entire Paleogene times. In fact, the complex architecture of seismic reflectors observed in the Paleogene Pabdeh series in the vicinity of the frontal triangle are more likely to result from Neogene tectonic imbrications rather than to represent intra-Paleogene unconformities and erosional truncations, the only proven erosional event occurring at the base of the Fars series (e.g. Jahani et al. 2009).

Due to these uncertainties, we prefer to label the four restoration stages comprised between Late Cretaceous and Miocene as Paleogene stages “a”, “b”, “c”, and “d”, respectively, rather than with absolute ages, as part of the related shortening could in fact still belong to the Late Cretaceous or already belong to the Late-Oligocene to Miocene contraction episodes.

Paleogene (?) to Late Miocene deformation was characterised by the progressive involvement of the Mesozoic platform in the deformed zone (Fig. 11c to f). The Hagab out-of-sequence thrust induced a progressive stacking of parautochthonous duplexes made up of the Musandam Platform carbonates. At shallower levels, the Hagab Thrust cut through the formerly emplaced Hawasina–Sumeini allochthon, with a triangle zone developing at the thrust front (Figs. 5, 10 and 11d). This led to the formation of promising large whaleback anticlines currently buried beneath the allochthon, adjacent parts of the foreland being also prone to collect oil and gas migrating from the platform.

Figure 11 also shows the subdivisions made in former time steps, in order to account for shorter (thinner) stratigraphic units in the section. Intermediate erosional surfaces and past topography are highly hypothetical. They have been tentatively adjusted here to fit the distribution of rock resistance to weathering and erosion, as well as additional constraints provided by Apatite Fission Track

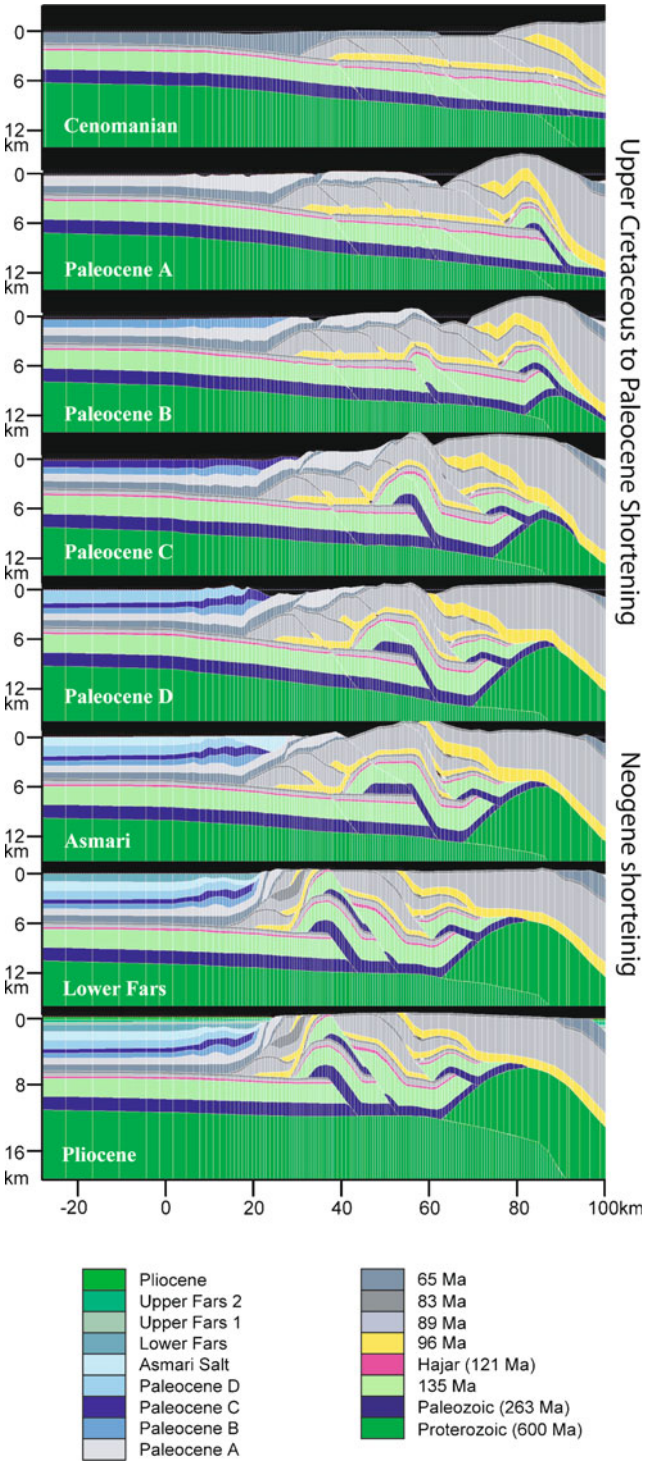

Fig. 11 Kinematic evolution of the Ceres model along the D4 section. the major shortening episode is dated as a continuum from Upper Cretaceous to Paleocene D. The Neogene episode is dated from Asmari to Lower Fars

data on the timing and value of the maximum burial (Naville et al. 2010, this volume; Tarapoanca et al. 2010, this volume). Similarly, the paleo-bathymetry is not always accurately constrained but we assume it has remained close to zero since the Late Maastrichtian (assuming that the Aruma foredeep was an overfilled basin, similar to the present Arabian Sea where average bathymetry is lower than 50 m, except near the Zagros thrust front where it is locally comprised between 50 and 100 m; Sindhu et al. 2007).

Further constraints on the paleo-burial and timing of the deformation

Paleo-burial is very well constrained in the foreland, where the entire sedimentary pile is well covered by seismic imagery, with limited erosion, and where calibration wells are available. In contrast, reconstructing the eroded thicknesses becomes more difficult in the foothills, where the main uncertainties relate to the timing and amount of maximum burial.

Erosional remnants such as a tectonic klippe made up of Hawasina material have been mapped at the top of the Musandam unit. Seemingly, Hawasina cherts are exposed at surface beneath the Musandam carbonates in the core of the Wadi Hagil tectonic window (Ellison et al. 2006), whereas Hawasina–Sumeini series have been drilled in wells of the Margham trend, implying a wide subsurface extent of the basinal allochthon toward the west, where it actually reaches or even extends farther than the Miocene tectonic front. The current northwestern limit of the Semail Ophiolite in the Dibba Zone constitutes also an erosional limit, precluding a direct control of its initial extent over the belt.

Fortunately, a number of apatite-bearing samples could be collected (1) in Triassic dolomites of the Musandam Platform; (2) in Turonian or younger clastic deposits of the Aruma Group still preserved in the Dibba Zone, both at the top of the Musandam carbonates and above the Sumeini slope facies; (3) in Paleozoic quartzites cropping out in exotic blocks of the Dibba mélange; as well as (4) in plagiogranites plugging both the base and the top of the Semail Ophiolite (Fig. 1; Tarapoanca et al. 2010 this volume; Naville et al. 2010, this volume). Cooling ages are comprised between 28 and 13 Ma in the Musandam Platform and Dibba Zone, implying the erosion of an up to 3 km-thick pile of Jurassic–Cretaceous carbonates and Hawasina allochthon during the Neogene. In contrast, apatite grains from plagiogranites of the Semail complex, provide evidences for an earlier unroofing of the ophiolite during the Late Cretaceous, with cooling ages of 72–76 Ma at the top of the ophiolite in the east, which are coeval and also consistent with the occurrence of paleo-soils, rudists and paleo-reefs on top of serpentinised ultramafics in the west (Woodcock and Robertson 1982; Hamdan 1990). Alternatively, younger cooling ages of 20 Ma have also been found at the base of the ophiolite near Masafi, in the core of the nappe anticline, thus accounting for a Neogene age for the refolding of the allochthon and stacking of underlying parautochthonous platform carbonate units.

Results of the Ceres fluid flow and pore-fluid pressure simulations

Lithology distribution is shown on Fig. 12a. The restoration was performed using a simplified lithologic model which did not integrate the subtle small scale layers on top of the platform. The individual layers within the Hawasina units were not taken into account either. The resulting porosity distribution is shown in Fig. 12b. The most interesting feature is the preservation of high porosity layers made up of mixed sand-shale (50%) within the anticlinal closures of the foreland basin. The sealing capacity of the Hawasina nappes is illustrated by the low porosity of its basal shaley layer (less than 6%), which is in agreement with field observations and the occurrence of hydraulic fractures in the Ausaq breccias at Jebel Gharaf, below the sole thrust of the Hawasina–Sumeini allochthon (Figs. 5, 8 and 9).

Water flow modelling results have been displayed on the evolutive cross-section (Fig. 13a) and emphasised for the major tectonic unit for both upper cretaceous and Jurassic reservoir rocks (Fig. 13b). The main units are the undisturbed foreland and the three main inverted part of the platform units sealed by the Hawasina and Sumeini nappes. Fluid flow evolution is illustrated by the fluid velocity evolution with time, which shows both the rapid change in motion associated to the main tectonic events, i.e. related to the thrust emplacement, and the long-term trend in direction of fluid flow, i.e. related to the major geodynamic changes such as the foredeep development.

Water flow pathways in the foreland basin

Water flow in the foreland basin is first controlled by long range updip lateral migration toward the foreland along the Mesozoic platform, and associated per ascensum migration toward the Pabdeh units (Fig. 13a). Subsequently, the development of the triangle zone forces a backward flow towards the inner units, updip of the Pabdeh layers which are back-tilted and thrust on top of the Hawasina–Sumeini allochthonous units which behave as a local indenter. As soon as the Asmari salt was deposited, lateral migration occurred below the salt, toward the anticlinal crests and the upper triangle zone. Thus, most of the fluids migrating vertically from the

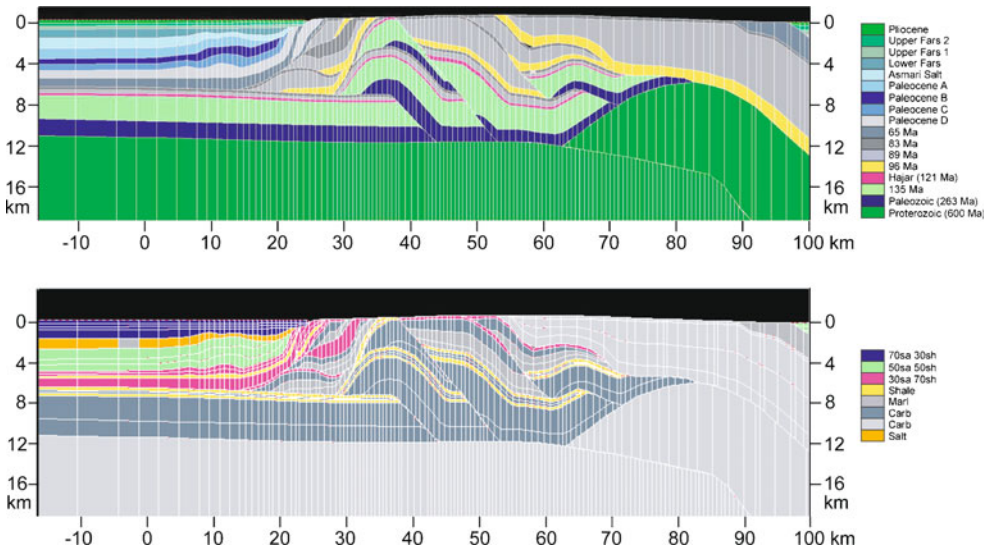

Fig. 12 Present-day section and lithology distribution of the D4 section. Lithology are composed of mixture of sandstone and shale end members for the clastic succession

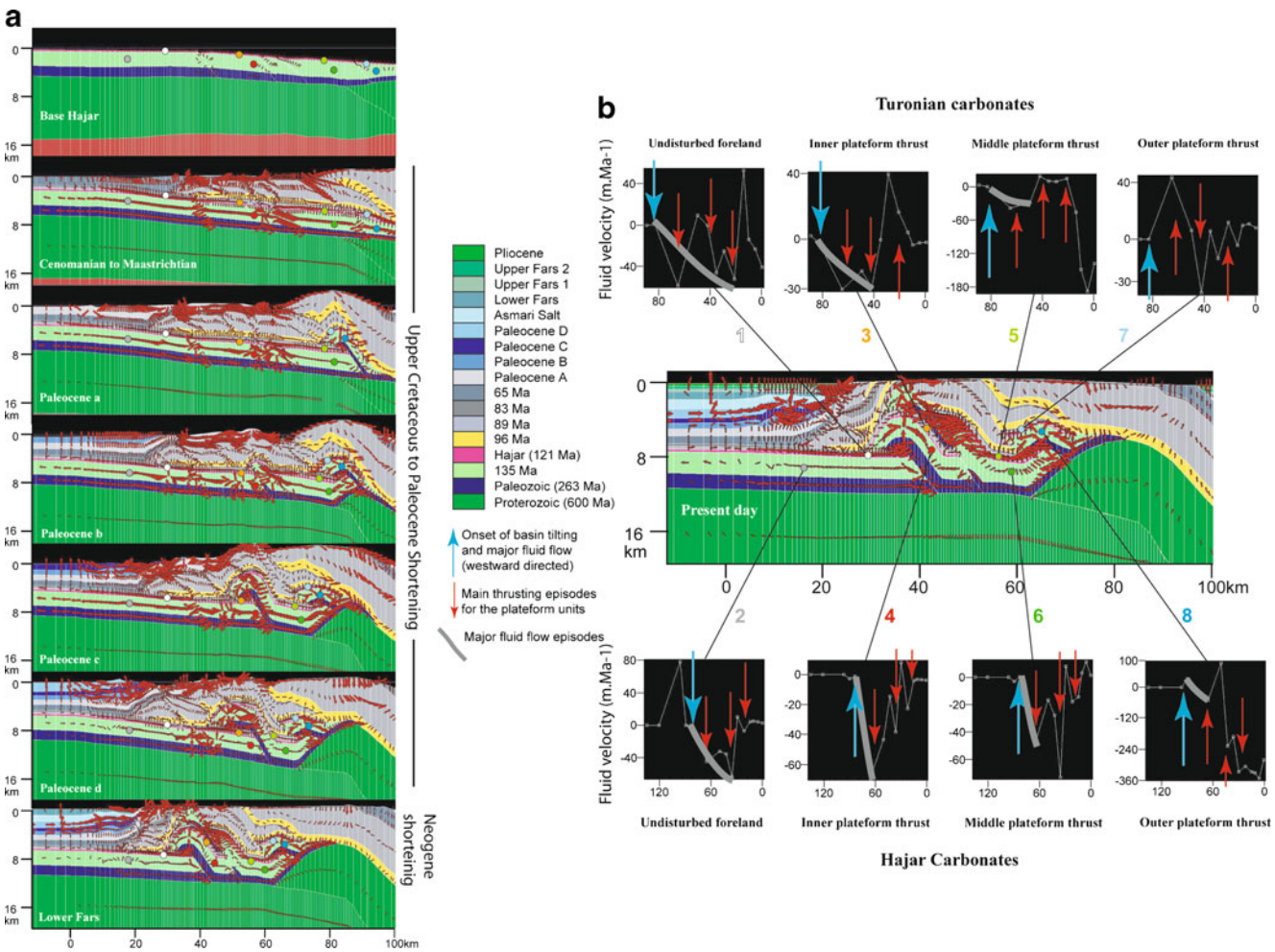

Fig. 13 **a** Time evolution of the Ceres fluid flow modelling for the water flow, shown on the lithology distribution from the Upper Paleozoic stage to Lower Fars Stage; **b** Present-day section and fluid flow, together with the time evolution of the horizontal fluid flow velocity for various cells located in the Paleozoic carbonates (*odd cells*) and in the Upper Cretaceous (*even cells*)

platform should be either collected by the disturbed foreland structures, or expelled toward the emerging thrusts of the triangle zone and, to a lesser extent, to the sub-thrust plays of the foothills.

Fluid flow pathways in the inner belt

Fluid flow within the thrust units is largely controlled during the early stage of deformation by the combined updip lateral migration in the platform and vertical per ascensum percolation across the Hawasina unit (Fig. 13a and b). The flexing of the margin and coeval LPS result in a rapid updip migration of the fluid forming a so-called squeegee episode, as already described in the Rocky Mountains as a low-flux, tectonically induced "hot flash" (Oliver 1986; Machel and Cavel 1999; Schneider 2003). The duration of the westward migration of fluid depends on the relative timing of the thrust activation. Early thrusting in the easternmost units shuts off the fluid migration in the deep Paleozoic and Cretaceous carbonates, whereas it is still active during Paleocene in the frontal units (Fig. 13b). This forelandward-directed flow of water is modified by the various thrusting episodes as illustrated by the major shifts in water velocity in Fig. 13b. This migration is even hidden for the eastern most thrusted unit of platformal carbonates for the Mesozoic carbonates.

As soon as the thrusts were activated, lateral pressure variations and anticlinal closures resulted in a migration of hydrocarbons toward the main anticlines (Fig. 13b). But this early flow pattern was dramatically modified by the late emplacement of deep platform duplexes (sub-thrust prospects), which may have developed partly synchronously with the shallower high-angle normal or transcurrent fault located along the southeastern border of the Musandam antiformal stack. In case this high-angle fault was pervious, the resulting opening of the system lead to a rapid expulsion toward the surface of the high temperature (hydrothermal) water and hydrocarbons formerly stored within connected parts of the deeper thrust units. The strong tilting of the triangle zone further west can also result in a rapid expulsion of fluids toward the surface along the major faults.

Discussions and conclusion

Petroleum system evolution

Known petroleum occurrences in the Emirates are consistent with the overall kinematic evolution of the D4 transect: during the early stages of foreland development (i.e., during Late Cretaceous–Paleogene times) long range hydrocarbon migration is evidenced by the current oil occurrences in the offshore part of the Emirates for hydrocarbon generated in the Mesozoic platform, updip along the regional foreland flexure. A more complex pattern of fluid flow and HC migration characterises the Neogene evolution of the foothills, with shorter fluid transfers. The occurrence of very efficient seals within the Cenozoic infill of the foredeep and tilting of frontal units account for local east-verging fluid migration in the vicinity of the frontal triangle zone. Short range, dominantly vertical migration could account for the recent filling of stratigraphic traps and growth anticlines below the salt, provided that mature source rocks actually still exist in the foredeep sequence. Alternatively, late condensate and gas generated within the Mesozoic source are also likely to fill the sub-thrust plays such as in the Margham and Sajaa fields (Blinton and Wahid 1983), in the areas where normal faults did not affect the overlying seals.

Diagenetic processes

Regional diagenetic processes which are likely to impact reservoir quality, can now be better understood in the frame of the Ceres fluid flow modelling, and replaced in the tectonic framework of the Northern Oman Mountains in seven evolutionary steps (e.g. Breesch 2008):

1. Permian to Early Cretaceous: during this pre-deformation stage, the Arabian margin was built up by a platform (current foreland and Musandam thrust unit), a slope (now part of the Sumeini allochthon) and a basinal domain (currently stacked within the Hawasina allochthon; Fig. 3). The Mesozoic, dominantly Jurassic–Lower Cretaceous platform carbonates was characterised by the development of synsedimentary dolomites and early hydraulic fractures originated by crack-sealing, prior to the development of burial stylolites. Deeper in the infra-Cretaceous strata the first generation of burial stylolites (BS1) were generated. The fluids responsible for the fracturing were over-pressured due to burial. They are characterised by local circulation, low salinities and host-rock buffered isotope signatures evidencing local remobilisation of formation fluids (Fig. 13a, Lower Cretaceous). During sea-level fluctuations and temporary emergences, eogenetic meteoric infiltration took place in the northern outcrops of the Musandam Platform.
2. Cenomanian (forebulge development and/or foreland inversions): obduction of the Oman–UAE ophiolites started SE of the study area, which resulted in the development of the Aruma foredeep and forebulge with meteoric water infiltration, as exemplified by the first karst phase in Wadi Batha Mahani. In the Sumeini

slope deposits, hydraulic fractures from the pre-BS period and burial stylolites were formed, followed by shear-related veins with calcite and quartz cement at a time burial stylolites already existed, but when tectonic stylolites (TS) did not yet develop. Meanwhile, BS1 development continued in the Musandam platform and affected also even the younger, i.e. Cretaceous reservoirs. During this phase, the major episode of squeegee fluid flow started with the updip motion of the deep platform formation fluid from the foredeep toward the hinterland.

3. Santonian–Campanian (Aruma foredeep development) to Paleocene (undated): thrust emplacement of the Sumeini, Hawasina and Semail ophiolite nappes took place (Fig. 13a). In the platform, no thrust faults were activated but burial fractures and a second generation of burial stylolites (BS2) was generated. In contrast to the far-travelled Hawasina–Sumeini allochthon, this stage was still part of the post-BS and pre-TS period in the Musandam platform. The thrusting caused deep burial locally in excess of 4500 m, even for Cretaceous reservoirs, with the development of a second generation of burial stylolites BS2 in the platform succession. Burial veins filled with white blocky calcite and ferroan saddle dolomite precipitated from warm geothermal fluids also formed during this stage, resulting from the updip squeegee fluid flow episode coming from the sedimentary series of the lower plate, by then underthrusted beneath the Hawasina–Semail allochthon which is well modelled by Ceres (Fig. 13b). In the Sumeini slope unit, the burial was less than in the underthrust foreland, being then limited to ±2000 m (to maximum 3000 m, Phillips et al. 2006) and the tectonic compression accounted for tectonic stylolite development. The farther to the east are located the thrusted units, the shorter the squeegee fluid flow event. This stage correspond to the larger temperature disequilibrium at depth, which is lowered vertically by the duration of the per ascensum displacement, unless it is tectonically controlled.
4. Post-deformational stage: a long period of tectonic relaxation and erosional unroofing started in the foothills domain, with continuous subsidence in the foreland basin, fluid expulsion and a continuous forelandward basinal fluid motion, but with a lower thermal disequilibrium. Zero or limited shortening occurred during this period, with continuous uplift and unroofing in the foothills, recorded by a thick pile of Paleogene deep-water clastics accumulated in the Gulf of Oman in the east, and in the residual foredeep basin, where the Pabdeh series accumulated.
5. Oligocene–Miocene (Asmari Fars sedimentation and out-of-sequence thrusting): Culmination of the Musandam unit occurred during the Miocene out-of-sequence activation of the Hagab and coeval accretion of deeper duplexes. First tectonic stylolites (TS1) develop in the Arabian platform and the fluid system with migration of hot brines along the steep reverse faults becomes active, resulting in syntectonic veins (e.g. from Wadi Ghalilah) and local dolomites (e.g. from Wadi Bih and Wadi Batha Mahani, see Fig. 13a, stage Lower Fars, and Fig. 14).
6. Present: uplift and erosion resulted in the present topography with meteoric infiltration and karstification in both the Musandam and Sumeini carbonates. In Wadi Batha Mahani, for instance, caves with stalagmites originate from this second karst phase. A fluid circuit with influence of meteoric fluids which resurface at moderate temperatures is inferred in the Musandam carbonates from rock samples collected in the vicinity of the Khatt's hot springs (Figs. 12a and 14).

Despite the Ceres modelling cannot yet handle local and long-term variations in the hydrodynamic properties of faults, it already provides realistic scenarios for both the lateral and vertical migration of fluids during the successive stages of the Arabian passive margin as well as during the subsequent evolution of the Oman thrust belt. Apart from the risks related to the maturity rank and distribution of the source rocks in the lower plate, the main uncertainties here for hydrocarbon prediction relates to the sealing capacity of the Hawasina–Sumeini allochthon, and to the long-term flow pattern along high-angle faults cross-cutting the entire

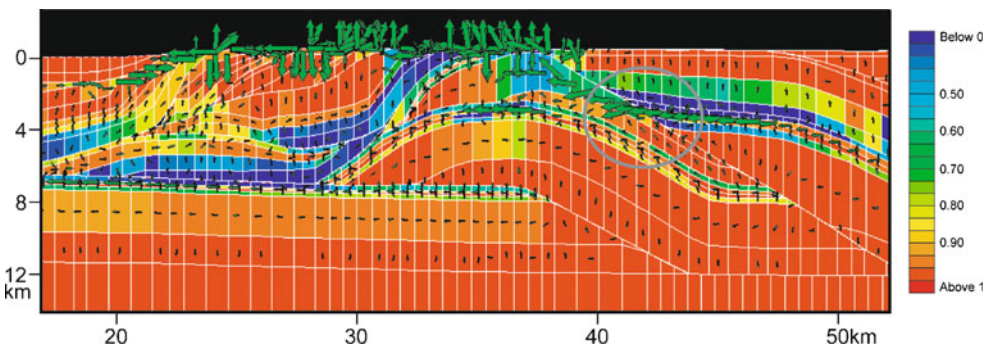

Fig. 14 Present-day distribution of water saturation (expressed as a percent of porosity occupied by water) with migration arrows, illustrating a challenging question that remains to be solved: When and why do high-angle faults act as permeability barriers or not?

allochthon (Fig. 14). Alternatively, a better knowledge of the chemistry of the fluids circulating along high-angle faults during the Cenomanian episode of foreland basin inversion would help, if combined with the results of such Ceres fluid flow modelling, to propose realistic estimates on the amount of platform limestones which could have been hydrothermally dolomitised, and hence the resulting average porosities of coeval potential reservoirs, as additional porosity probably developed during such vertical escape of diagenetic fluids.

Acknowledgements We acknowledge Saleh Al Mahmoudi, Khalid Al Hosani, Abdullah Gahnoog and the Ministry of Energy of the UAE for their long-term support during this project and authorising this publication. Patrick Le Foll and Denis Deldique are thanked for expertise in figure preparation.

References

Alsharhan AS (1989) Petroleum geology of the United Arab Emirates. J Petrol Geol 12:253–288

Benchilla L, Guilhaumou N, Mougin P, Jaswal T, Roure F (2003) Paleoburial and pore pressure reconstruction of reservoir rocks in foothills areas: a sensitivity test in the Hammam Zriba (Tunisia) and Koh-I-Maran (Pakistan) ore deposits. Geofluids 3:103–123

Blinton JS, Wahid IA (1983) A review of Sajaa field development, Sharjah. United Arab Emirates, 3rd Middle East Oil Show, SPE Bahrain, pp. 601–606

Boote DRD, Mou D, Waite RI (1990) Structural evolution of the Suneinah foreland, Central Oman Mountains. In: Robertson AHF, Searle MP, Ries AC (eds) The geology and tectonics of the Oman region, Special Publication, 49. Geological Society, London, pp 397–418

Breesch L (2008) Diagenesis and fluid system evolution in the Northern Oman Mountains, UAE. PhD Thesis, KU Leuven, Belgium, 159 p

Breesch L, Swennen R, Vincent B (2006) Dolomite formation in breccias at the Musandam Platform border, Northern Oman Mountains, UAE. J Geochem Explor 89(1–3):19–22

Breesch L, Swennen R, Dewever B, Mezini A (2007) Deposition and diagenesis of carbonate conglomerates in the Kremenara anticline, Albania: a paragenetic time marker in the Albanian foreland fold-and-thrust belt. Sedimentology 54(3):483–496

Breesch L, Swennen R, Vincent B (2009) Fluid flow reconstruction in hanging and footwall carbonates: compartmentalization by Cenozoic reverse faulting in the Northern Oman Mountains (UAE). Mar Petrol Geol 26(1):113–128

Breesch L, Swennen R, Vincent V, Ellison RA, Dewever B (2010a) Dolomite cementation and recrystallisation of sedimentary breccias along the Musandam Platform margin (UAE). J Geochem Explor 106(1–3):34–43

Breesch L, Swennen R, Dewever B, Roure F, Vincent B (2010b) Diagenesis and fluid system evolution in the Northern Oman Mountains. Implications for petroleum exploration, UAE, in review

Callot JP, Roure F (2007) Petroleum systems appraisal and Ceres modelling of the Emirates D4 section. Ministry of Energy, UAE-IFP report

Dunne LA, Manoogian PR, Pierini DF (1990) Structural style and domains of the Northern Oman Mountains (Oman and United Arab Emirates). In: Robertson AHF, Searle MP, Ries AC (eds) The geology and tectonics of the Oman region, Special Publication, 49. Geological Society, London, pp 375–386

Eilrich B, Grötsch J (2003) The Lower Cretaceous carbonate slope-to-platform-margin succession near Khatt, United Arab Emirates: sedimentary facies and depositional geometries. GeoArabia 8 (2):275–294

Ellison RA, Woods MA, Pickett EA, Arkley SLB (2006) Geology of the Al Rams 1:50 000 map sheet, 50-1, United Arab Emirates. British Geological Survey, Keyworth, p 42

Ellison RA, Phillips ER, Styles MT (2009) A geostraverse across the Late Cretaceous fold and thrust belt of the UAE: from ophiolite to platform margin. Guide for Dibba Zone field excursion, ILP Task Force on Sedimentary Basin, BGS-Ministry of Energy of the UAE, p. 31

Faille I, Nataf F, Schneider F, Willien F (1998) Domain decomposition methods for fluid flows in porous medium: ECMOR, 6th European Conference on the Mathematics of Oil Recovery, Peebles, September 8–11, 1998, Proceedings, Paper B-06, p. 6

Ferket H, Ortuño S, Swennen R, Roure F (2003) Diagenesis and fluid flow history in reservoir carbonates of the Cordilleran fold- and thrust- belt: The Cordoba Platform. In Bartolini C, Burke K, Buffler R, Blickwede J, Burkart B (eds) Mexico and the Caribbean region: plate tectonics, basin formation and hydrocarbon habitats, AAPG Memoir 79, Ch. 10, pp. 283–304

Ferket H, Swennen R, Ortuño-Arzate S, Cacas MC, Roure F (2004) Hydrofracturing in the Laramide foreland fold-and-thrust belt of Eastern mexico. In: Swennen R, Roure F, Granath J (eds) Deformation, fluid flow and reservoir appraisal in foreland fold-and-thrust belts, vol. 1. AAPG Hedberg, Memoir, pp 133–156

Glennie KW, Boeuf MGA, Hughes-Clarke MW, Moody SM, Pilaar WFH, Reinhardt BM (1974) Late Cretaceous nappes in Oman Mountains and their geologic evolution. AAPG Bull 57:5–27

Graham GM (1980a) Evolution of a passive margin, and nappe emplacement in the Oman Mountains. In Panayiotou A (ed.), Proceedings, International Ophiolite Symposium, Cyprus, 1979, pp. 414–423

Graham GM (1980b) Structure and sedimentology of the Hawasina window, Oman Mountains. PhD Thesis. Open University, UK

Hamdan ARA (1990) Maastrichtian Globotruncanids from the western front of the northern Oman Mountains: implications for the age of post-orogenic strata. J Fac Sci, United Arab Emirates Univ 2:53–66

Hanna SS (1986) The Alpine (late Cretaceous and Tertiary) tectonic evolution of the Oman Ranges: a thrust tectonic approach. In OAPEC/Symposium on the hydrocarbon potential of intense thrust zones, vol. 2. Abu Dhabi, pp. 125–174

Hanna SS (1990) The Alpine deformation of the Central Oman Mountains. In: Robertson AHF, Searle MP, Ries AC (eds) The geology and tectonics of the Oman region, Special Publication, 49. Geological Society, London, pp 341–359

Jahani S, Callot JP, Letouzey J, Frizon de Lamotte D (2009) The eastern termination of the Zagros fold-and-thrust belt, Iran: structures, evolution, and relationships between salt plugs, folding and faulting. Tectonics, doi:10.1029/2008TC002418, 2009

Lacombe O, Malandain J, Vilasi N, Amrouch K, Roure F (2009) From paleostresses to paleobutrial in fold–thrust belts: preliminary results from calcite twin analysis in the outer Albanides. In The geology of vertical movements of the lithosphere, vol. 475. Tectonophysics, pp. 128–141, doi:10.1016/j.tecto.2008.10.023

Lippard SJ, Smewing JD, Rothery DA, Browning P (1982) The geology of the Dibba Zone, northern Oman Mountains; a preliminary study. J Geol Soc Lond 139:59–66

Machel HG, Cavell PA (1999) Low-flux, tectonically-induced squeegee fluid flow ("hot flash") into the Rocky Mountain foreland basin. Bull Canadian Petrol Geol 47:510–533

Naville C, Ancel M, Andriessen P, Ricarte P, Roure F (2010) New constrains on the thickness of the Semail Ophiolite in the Northern Emirates. This volume

O'Donnell GP, Daly CB, van Mount S, Krantz RW (1994) Seismic modelling over the Margham field, Dubai, United Arab Emirates. In: Al Husseini MI (ed) GEO'94, vol. II. The Middle East Petroleum Geosciences, Bahrain, pp 737–746

Oliver J (1986) Fluid expelled tectonically from orogenic belts: their role in hydrocarbon migration and other geologic phenomena. Geology 14:99–102

Patton TL, O'Connor SJ (1986) Cretaceous flexural history of the northern Oman Mountain foredeep, United Arab Emirates. In Hydrocarbon potential of intense thrust zones, vol. 1. Abu Dhabi Conference, pp. 75–120

Patton TL, O'Connor SJ (1988) Cretaceous flexural history of northern Oman Mountain foredeep. United Arab Emirates. AAPG Bull 72:797–809

Phillips ER, Ellison RA, Farrant AR, Goodenough KM, Arkley SLB, Styles MT (2006) Geology of the Dibba 1:50 000 map sheet, 50-2, United Arab Emirates. British Geological Survey, Keyworth, p 59

Ricateau R, Riché PH (1980) Geology of the Musandam peninsula (Sultanate of Oman) and its surroundings. J Petrol Geol 3 (2):139–152

Robertson AHF, Blome CD, Cooper DWJ, Kemp AES, Searle MP (1990) Evolution of the Arabian continental margin in the Dibba Zone, Northern Oman Mountains. In: Robertson AHF, Searle MP, Ries AC (Eds), The geology and tectonics of the Oman region. Geol. Soc. Spec. Publ. 49, pp. 251–284

Roure F (2008) Foreland and hinterland basins: What controls their evolution? Swiss Journal of Geosciences, Birkhaüser Verlag, Basel, doi:10.1007/s00015-008-1285-x

Roure F, Swennen R, Schneider F, Faure JL, Ferket H, Guilhaumou N, Osadetz K, Robion PH, Vendeginste V (2005) Incidence and importance of Tectonics and natural fluid migration on reservoir evolution in foreland fold-and-thrust belts. In: Brosse E et al (eds) Oil and Gas Science and Technology, Oil and Gas Science and Technology, Revue de l'IFP, 60, 67–106

Roure F, Andriessen P, Breesch L, Broto K, Bruneau J, Chérel L, Collin M, Ellouz N, Faure JL, Guilhaumou N, Jardin A, Muller C, Naville CH, Ricarte P, Rodriguez S, Swennen R, Tarapoanca M (2006) Deep seismic survey in the Northern Emirates, Part II: Main interpretation and modelling report. Ministry of Energy, UAE-IFP Report n° 59 359, p. 125

Roure F, Cloetingh S, Scheck-Wenderoth M, Ziegler P (2009) Achievements and challenges in sedimentary basins dynamics. In: Cloeting S, Negendank G (eds) International Year of Planet Earth, Special Volume on Deep Earth, Chaper 5. Springer

Roure F, Callot JP, Ferket H, Gonzales E, Guilhaumou N, Lacombe O, Malandain J, Mougin P, Swennen R, Vilasi N (2010) The use of paleo-thermo-barometers and coupled thermal, fluid flow and pore fluid pressure modeling for HC and reservoir prediction in Fold and Thrust belts. In: Goffey GP, Craig J, Needham T, Scott R (eds) Hydrocarbons in Contractional Belts. Geological Society, London, Special Publications 348, pp. 87–114, doi:10.1144/SP348.6

Sassi W, Rudkiewicz JL (2000) Computer modelling of petroleum systems along regional cross-sections in foreland fold and thrust belts. In Geology and Petroleum Geology of the Mediterranean and Circum Mediterranean Basins, Malta, Proceedings, Extended Abs., C27–1–4

Schneider F (2003) Basin modelling in complex area: examples from eastern Venezuelan and Canadian foothills. Oil Gas Sci Technol Revue de l'IFP 58(2):313–324

Schneider F, Devoitine H, Faille I, Flauraud E, Willien F (2002) Ceres2D: a numerical prototype for HC potential evolution in complex area. Oil Gas Sci Technol Revue de l'IFP 57(6):607–619

Searle MP (1985) Sequence of thrusting and origin of culminations in the northern and central Oman mountains. J Struct Geol 7:129–143

Searle MP (1988a) Thrust tectonics of the Dibba Zone and the structural evolution of the Arabian continental margin along the Musandam Mountains (Oman and UAE). J Geol Soc London 145:53–63

Searle MP (1988b) Structure of the Musandam culmination (Sultan-ate-of-Oman and United-Arab-Emirates) and the Straits of Hormuz Syntaxis. J Geol Soc 145:831–845

Searle MP, James NP, Calon TJ, Smewing JD (1983) Sedimentolog-ical and structural evolution of the Arabian continental margin in the Musandam Mountains and Dibba Zone, United Arab Emirates. Geol Soc Am Bull 94(12):1381–1400

Sindhu B, Suresh I, Unnikrishnan AS, Bhatkar NV, Neetu S, Michael GS (2007) Improved bathymetric datasets for the shallow water regions in the Indian Ocean. J Earth Syst Sci 116: 261–274

Styles MT, Ellison RA, Arkley SLB, Crowley Q, Farrant A, Good-enough KM, McKervey JA, Pharaoh TC, Phillips ER, Schofield D, Thomas RJ (2006) The geology and geophysics of the United Arab Emirates. British Geological Survey, Keyworth

Swennen R, Muska K, Roure F (2000) Fluid circulation in the Ionian fold and thrust belt (Albania): Implications for hydrocarbon prospectivity. J Geochem Explor 69:629–634

Swennen R, Roure F, Granath J (eds) (2004) Deformation, fluid flow and reservoir appraisal in foreland fold and thrust belts. AAPG Hedberg Series, Memoir 1, p. 430

Tarapoanca M, Andriessen P, Broto K, Chérel K, Ellouz-Zimmerman N, Faure JL, Jardin A, Naville C, Roure F (2010) Forward kinematic modelling of a regional transect in the Northern Emirates, using apatite fission track age determinations as constraints on paleo-burial history. This volume

Van Geet M, Swennen R, Durmishi C, Roure F, Muchez Ph (2002) Paragenesis of Cretaceous to Eocene carbonate reservoirs in the Ionian foreland fold-and-thrust belt (Albania): Relation between tectonism and fluid flow. Sedimentology 49:697–718

Vandeginste V, Swennen R, Gleeson SA, Ellam RM, Osadetz K, Roure F (2005) Zebra dolomitization as a result of focused fluid flow in the Rocky Mountains Fold-and-Thrust belt, Canada. Sedimentology 52:1067–1095

Vilasi N (2003) Caractérisation des paléofluides et reconstruction de l'histoire de l'enfouissement et de la température de réservoirs pétroliers dans la chaîne d'Oman et son avant-pays. Master, Univ. Paris VI

Vilasi N, Malandain J, Barrier L, Callot JP, Guilhaumou N, Lacombe O, Muska K, Roure F, Swennen R (2009) From outcrop and petrographic studies to basin-scale fluid flow modelling: the use of the Albanian natural laboratory for carbonate reservoir characterization. Tectonophysics 474:367–392

Warburton J, Burnhill TJ, Graham RH, Isaac KP (1990) The evolution of the Oman Mountains foreland basin. In: Robertson AHF, Searle MP, Ries AC (eds) The geology and tectonics of the Oman region, Special Publication, 49. Geological Society, London, pp 419–427

Watts KF (1990) Mesozoic carbonate slope faciès marking the Arabian platform margin in Oman : depositional history, morphology and palaeogeography. In: Robertson AHF, Searle MP, Ries CA (eds) The geology and tectonics of the Oman region, Geol. Soc. Spec. Publ., 49, 139–160

Watts KF, Blome CD (1990) Evolution of the Arabian carbonate platform margin slope and its response to orogenic closing of a Cretaceous ocean basin, Oman. In Evolution of carbonate platforms, International Association Sedimentary, Special Publication, 9, pp. 291–323

Watts KF, Garrison RE (1986) Sumeini Group, Oman-, evolution of a Mesozoic carbonate slope on a South Tethyan continental margin. Sed Geol 48:107–168

Woodcock NH, Robertson AHF (1982) Stratigraphy of the Mesozoic rocks above the Semail Ophiolite, Oman. Geol Mag 119:67–76